DRA

aer

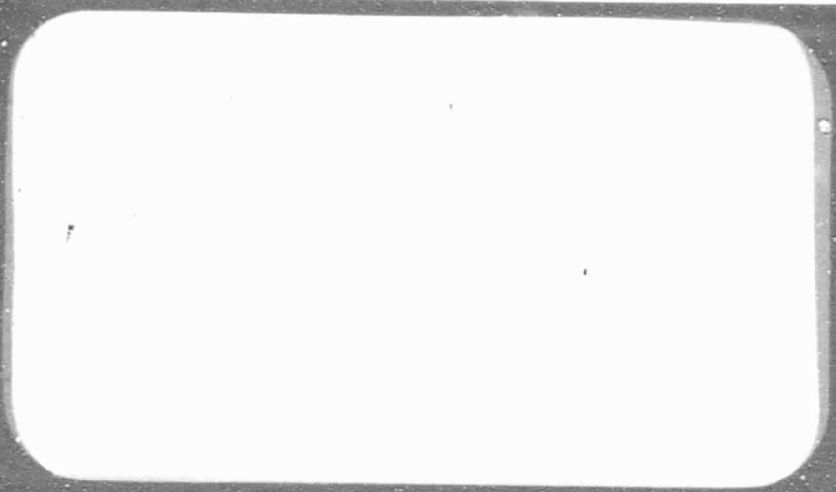

ATMOSPHERIC AND ENVIRONMENTAL RESEARCH, INC.
CAMBRIDGE, MASSACHUSETTS

NEW MARTIAN SATELLITE SEARCH

Final Report for Period
June 1, 1980 to May 31, 1983

Prepared for

NASA Headquarters
Washington, D.C. 20546

Prepared by

William H. Smyth
Atmospheric and Environmental Research, Inc.
840 Memorial Drive
Cambridge, MA 02139

TECHNICAL REPORT STANDARD TITLE PAGE

1. Report No.	2. Government Accession No.	3. Recipient's Catalog No.

4. Title and Subtitle	5. Report Date
New Martian Satellite Search	May 1983
	6. Performing Organization Code
7. Author(s) William H. Smyth	8. Performing Organization Report No.
9. Performing Organization Name and Address Atmospheric and Environmental Research, Inc. 840 Memorial Drive Cambridge, Massachusetts 02139	10. Work Unit No.
	11. Contract or Grant No. NASW-3399
	13. Type of Report and Period Covered Final Report June 1, 1980-May 31, 1983
12. Sponsoring Agency Name and Address NASA Headquarters Contracts and Grants Division Washington, DC 20546	14. Sponsoring Agency Code HWC-2

15. Supplementary Notes

16. Abstract

The approach pictures taken by the Viking 1 and Viking 2 spacecrafts two days before their Mars orbital insertion maneuvers, were analyzed in this Mars data analysis project in order to search for new satellites within the orbit of Phobos. To accomplish this task, a complete search procedure and analysis strategy were formulated, developed and executed using the substantial image processing capabilities of the Image Processing Laboratory at the Jet Propulsion Laboratory. The development of these new search capabilities should prove to be valuable to NASA in processing of image data obtained from other spacecraft missions. The result of applying the search procedures to the Viking approach pictures was as follows: no new satellites of comparable size (~20 km) and brightness to Phobos or Demios were detected within the orbit of Phobos.

17. Key Words (Selected by Author(s))	18. Distribution Statement
satellites Mars Viking spacecrafts	UNLIMITED

19. Security Classif. (of this report)	20. Security Classif. (of this page)	21. No. of Pages	22. Price*
Unclassified	Unclassified	57	

*For sale by the Clearinghouse for Federal Scientific and Technical Information, Springfield, Virginia 22151.

Figure 2. Technical Report Standard Title Page

TABLE OF CONTENTS

I. INTRODUCTION

The objective of this Mars data analysis project has been to search the Viking 1 and Viking 2 approach pictures for new satellites. In executing this objective, the project has utilized the substantial image processing capabilities of the Image Processing Laboratory (IPL) at the Jet Propulsion Laboratory, the support for which was supplied separately by NASA Headquarters.

The original interest in pursuing this project came from data obtained on April 8, 1976 by McCook (1979) who observed the Mars occultation of the star Epsilon Geminiorum. Initial examination of this ingress light curve, recorded at the observatory of Villanova University, showed an intensity drop to total occultation of the light of the star for about 0.7 seconds with no apparent change in the background light level coming from Mars. This change was associated with some occurence in the near-Mars environment and was tentatively interpreted as an occultation of the star light by a close Martian satellite with perhaps an 8 to 15 km diameter. A later and more careful interpretation of other occultation data (French, Goguen, Duthie, 1978; Liller, et al., 1978; French and Elliot, 1979) revealed that a similar signature was also seen by other observers, but that the signature was most likely caused by large-scale structures in the Mars atmosphere of large horizontal extent (French and Elliot, 1979).

In order to search the Viking 1 and Viking 2 approach pictures for new satellites, a complete search procedure and analysis strategy had to be formulated, developed and executed. Since no such capability existed at IPL, a considerable effort was undertaken in this project to create this needed capability. The search procedure so developed can be divided into three parts (1) screening of the image data to obtain initial satellite candidate objects, (2) navigation processing of the candidate object data, and (3) analysis of the candidate object data. Each of these parts is described in detail in Section 3. The most difficult task was that of developing the image processing techniques for the correlation analysis of candidate objects in part 3. This development, however, provided some rather sophisticated software tools and

capabilities that should prove to be valuable to NASA in processing of image data obtained from other spacecraft missions.

The result of applying the search procedure to the Viking approach pictures was as follows: no new satellites of comparable size (~20 km) and brightness to Phobos or Deimos were detected within the orbit of Phobos. Probing the approach pictures for satellite significantly smaller or dimmer than Phobos was not possible because the exposure times for the pictures were adjusted to properly image Mars (an extended object) and were not set at their maximum values as would be optimum for detection of new satellites.

II. DESCRIPTION OF THE VIKING APPROACH PICTURES

The Viking 1 and Viking 2 spacecrafts, respectively, were launched on 20 August and 9 September in 1975 and initiated their Mars orbital insertion maneuvers on 19 June (i.e., day 171 of the year) and 7 August (i.e., day 220 of the year) in 1976. Two days prior to the Viking 1 orbital insertion maneuvers (i.e., days 169 and 170), nineteen sequences of pictures were taken in two or three colors by the two vidicon cameras. Two days prior to the Viking 2 orbital insertion maneuvers (i.e., days 218 and 219), eighteen sequences of pictures were taken in three colors by the two vidicon cameras. These approach pictures contained all or some fraction of the half-illuminated disc at Mars. They also contained projected views on the image plane of a significant region of the surrounding circumplanetary space (image-plane displacements from the planet center varying from 17,000 km to 8,000 km for Viking 1 and from 18,000 km to 7,000 km for Viking 2). One of the Viking 1 approach pictures, illustrating the image-plane view of the camera, is shown in Figure 1.

The two known satellites of Mars, Deimos and Phobos, have essentially circular orbits that lie nearly in the equatorial plane of the planet and have orbital radii of about 23,000 km and 9,300 km respectively. During the time that the approach pictures were taken, both spacecrafts were located above south Mars latitudes between 30° and 36° so that their cameras imaged the space that was almost always well within the nearly equatorial orbit of Deimos and many times well within the nearly equatorial orbit of Phobos (see Figure 1). The approach pictures therefore imaged a region of circumplanetary space about Mars suitable to search for new satellites near are within the orbit of Phobos. Since the orbital period of Phobos is 7.64 hours and the period of an object with a circular orbital radius of 4000 km (slightly larger than the 3393 km equatorial radius of Mars) is 2.13 hours, the approach pictures taken mostly at two-hour intervals also have well placed time windows in which to detect new satellite within the orbit of Phobos.

The approach pictures for Viking 1 and Viking 2 are each labeled by a unique picture number (PIC. NO.). The picture number is composed

of a three-digit number (denoting the day of the year on which the picture was taken) followed by a letter (C for Viking 1 and D for Viking 2) and finally followed by a sequence number of two digits initialized to 01 at the beginning of a new day. The picture numbers for each approach picture and some other relevant picture information taken from the Viking SEDR (supplementary experimental data records) are given in Table 1 and Table 2 for Viking 1 and Viking 2, respectively. For Viking 1, two non-smeared approach pictures 168C09 and 168C11 taken a day earlier than those catalogued in Table 1 as well as picture 169C03 that is listed in Table 1 were mistakenly not included in our study.

From Table 1 and Table 2, the distance of the spacecrafts from Mars during the approach picture exposures can be seen to vary between about 700,000 km and 200,000 km. The exposed area on the image plane is 1056 pixels vertically (the line value L) and 1182 pixels horizontally (the sample value S). The equivalent spatial pixel resolving power of the image, the expected size of Phobos and the absolute brightness of Phobos for these spacecraft distances from Mars are summarized in Table 3. A nominal diameter of Phobos of 20 km was adopted in Table 3 and differs a little from the actual ellipsoid radial dimensions in kilometers of (13.5, 10.5, 9.0). The full size of Phobos would vary from about one pixel to several pixels, but since it is only about half illuminated by the sun, its image signature will appear even smaller.

The response of the Viking camera to a point light source is to spread the signal from the central pixel to the adjacent pixels so as to increase the image size of the point while reducing its absolute brightness per pixel. Phobos, or an object of equivalent brightness, should thus produce a distinct several pixel signature on the picture image if the exposure time and filter transmission factor (i.e., determined by the filter color selected, see Table 4) are such to allow a sufficient signal to noise level to be captured. From Table 1 and Table 2, both the exposure time and filter color can be seen to vary from picture to picture. The distribution and relative sensitivities of these approach pictures are summarized in Table 5, from which it may be seen that the Viking 1 pictures are significantly more sensitive

than the Viking 2 pictures. For Phobos, or an equivalently bright satellite, the albedo and the photometric function of its surface further reduces the absolute camera response of Table 4 by an amount which is approximately the same for each filter. The ability of the cameras to detect Phobos in the approach pictures will be assessed and shown in the following section to be possible, unfortunately, only for a small subset of the total pictures in Table 1 and Table 2. This occurs primarily because the camera exposure values were selected to properly image Mars (an extended object) and were necessarily significantly lower than the maximum exposure times of 2660 msec that would be optimum for identifying new satellites.

III. SATELLITE SEARCH PROCEDURE AND ANALYSIS

3.1 Introduction

In order to utilize the Viking 1 and Viking 2 approach pictures listed in Table 1 and Table 2 to search for new satellites, a search procedure and analysis had to be formulated and all necessary image processing software tools had to be developed. This formulation and development phase of the project represented a considerable effort. It was undertaken at the IPL facility of the Jet Propulsion Laboratory (JPL) by Gary Yagi and was supervised by W.H. Smyth of AER. One of the direct and positive contributions of this project has been the development of a satellite search capability for IPL. This capability may prove to be useful in processing of image data from other NASA spacecraft missions.

The satellite search procedure and analysis has been divided into three steps: (1) screening of the image data to produce an initial candidate object list, (2) first order navigation processing of the candidate object data, and (3) analysis of the candidate object data. All numerical computations required in this effort were performed on the IBM 370/158 computer at IPL and ran under VICAR, the JPL image processing language and its associated application programs. In addition to application programs under VICAR, many new application programs were created, the most difficult of which were those needed for the prograde and retrograde orbit correlational analysis in step three.

3.2 Screening of the Image Data

This first step in the search procedure and analysis is diagramatically illustrated in Figure 2 and will be discussed in detail below. The approach pictures are obtained in digital form from the Viking Orbiter EDR (experimental data record) data which are stored on computer tapes. In order to search for the pixel signature of possible satellite candidate objects, a VICAR program was utilized to determine the medium background level above which a candidate object could be identified. The background filter chosen for this utilized an 11 x 11 pixel area to define the medium background at each pixel image location.

Any object that was then two or more adjacent pixels in size with a brightness of 4 DN or more above this background level was classified as a possible candidate object. A VICAR program was then applied to the digital image data to identify and locate the coordinates of the centroid of each candidate object in the pixel coordinates (L,S) of image space (the geometrically uncorrected image plane). The collection of these candidate object coordinates for each approach picture was then stored on a disc file (see Figure 2).

Many objects that are identified by the object locater were camera blemishes, reseau (uniformly spaced points on the image plane) or local maximums that occur in the camera system and therefore need to be screened from the candidate list. Other objects occurring on the disc of Mars as bright spots also need to be so identified and removed from the candidate list. Finally transmission errors and other spurious signals need to be properly identified and deleted from the candidate list. To accomplish this, two methods were applied. A blemish filter program, which compared known camera blemish patterns with the objects in the candidate list, was written and applied to the candidate list file. A computer printout of the pixel listing of each object that succeeded in passing through this blemish filter was then obtained. Parallel to this, VICAR programs were used to obtain photographs of all approach pictures containing candidate objects with each candidate object identified on the photograph. One such photograph for the Viking 1 and Viking 2 approach pictures is shown in Figure 3 and Figure 4, respectively. Visual examination of the photographs and pixel listings was then used to manually screen from the candidate list unsuitable objects. Objects remaining after this screening process define the initial candidate object list for the second stage of processing.

The screening process provided 54 initial candidate objects for the Viking 1 approach pictures and 355 initial candidate objects for the Viking 2 approach pictures. The Viking 2 approach pictures contain more than six times as many initial candidate objects as Viking 1. This resulted because both the gradient in the absolute background DN-value as well as the noise fluctuation about this background value were significantly larger in the Viking 2 approach pictures than those in the Viking 1 approach pictures. This difference in the background gradient can, for example, be seen by comparing Figure 3 and Figure 4.

In addition to this screening processing, each photograph of the approach pictures that still contained candidate objects was used to manually measure the pixel location of the planet center (see Figure 2). This information is vital to locate the vector direction of the optical axis of each image which is inaccurately supplied by the cone and clock angles in the SEDR. This inaccuracy results from the limit cycle of the spacecraft (the uncertainty in the vector orientation of the spacecraft that is controlled within a specified tollerance by the use of small control jets).

3.3 First Order Navigation Processing of Candidate Object Data

Additional processing is required before the objects in the initial candidate list can be properly analyzed. This additional processing is diagramatically illustrated in Figure 5 and involves both geometric correction of the images and navigation (assembly of all spacecraft, planet, ephemeris, camera and candidate object information into a coherent whole).

The information obtained in step one (see Figure 2) was used as input and was manually assembled and organized in a file containing the image space coordinate of the initial candidate objects and the planet center for each relevant approach picture (see Figure 5). Using a file containing the nominal (i.e., average) locations of the reseau markings of the camera, a first order geometric correction was applied to all the image space (L,S) coordinates of the initial candidate objects and planet centerr. These geometrically corrected coordinates are then called the object space (L,S) coordinates of the initial candidate objects and planet centers.

Using the Viking SEDR files and application programs developed for the Voyager spacecraft, the navigation of each image is accomplished and the orientation information for the spacecraft, planet, camera as well as the object space coordinates of the initial candidate objects is placed in a MIDS (Mars Intermediate Data Set) computer file. The MIDS file contains all input information necessary for further analysis of the pictures. A complete list of all the initial candidate objects together with their picture number and their object space (L,S) coordinates is given in Table 6 and Table 7 for the Viking

1 and Viking 2 approach pictures, respectively. Additional information describing the pixel characteristics, size and brightness of the initial candidate objects is also included in Table 6 and Table 7 for convenience. Much of this additional information was, however, determined later in the analysis described below.

3.4 Analysis of Candidate Object Data

The analysis of the initial candidate objects list to search for new satellites can be divided into (1) a simple global search for background stars and spatial clustering of candidate objects and (2) a more complex satellite correlation analysis of the individual candidate objects. The global search was performed by properly aligning the planet centers of all picture frames and properly projecting and superimposing all candidate objects onto one image plane. This process revealed nothing more than a random distribution of the initial candidate object points on the composite image plane. This implies that most of the initial candidate objects are random noise and that any star in the field of view was too dim to be imaged. The likely magnitude of any star in the field of view should be no more than fifth or sixth magnitude which is considerably dimmer than the near zeroth magnitude expected for Phobos (see Table 3). A more complex satellite correlation analysis, discussed below, was then developed and applied to the Viking 1 and king 2 candidate object data separately.

The correlation analysis search for satellites is based upon the assumption that any real satellite will move about Mars in accordance with the gravitational inverse-square force law for the planet. The object space (L,S) coordinates of those candidate objects occurring in different approach pictures that actually correspond to a real satellite should therefore coincide when they are dynamically transformed to a common time frame. A significant effort was expanded to develop the application programs suitable to perform this correlation analysis. The scope of correlation analysis was restricted to circular orbits in the equatorial plane of Mars. This restriction was imposed for two reasons. First, the method could be tested and perfected by locating the satellite Phobos which has a nearly circular

prograde orbit within about one degree of the equatorial plane. Second, development and execution of the more general out-of-the-equatorial-plane correlation analysis, although initiated, was soon realized to be beyond the time and funding limits of this project.

Having restricted the satellite correlation analysis to circular orbits in the equatorial plane of Mars, the object space (L,S) coordinates for each candidate object were projected along the optical axis of the camera to obtain a unique radius r and longitude θ for that object. Errors in determining the (r,θ)-values exactly arose primarily because of the inability to measure the center of Mars exactly. The existence of this uncertainty in the (r,θ)-value was necessarily incorporated in the analysis. The resulting distribution in the radii of the circular orbits of the initial candidate objects, in 1000 kilometer wide intervals in the equatorial plane, is summarized in Table 8. In Table 8, three of the Viking 2 candidate objects (number 40, 41 and 206 in Table 7) have projections that are actually inside of the equatorial radius of Mars (3393 km).

To minimize the propagation of measurement uncertainties in the (r,θ) values for each candidate point in the satellite correlation analysis, a two-dimensional ideal space (R,Θ) is introduced (at a reference time t_o midway in the Viking approach picture time sequence) for searching and correlation display purposes. A computer search through this two-dimensional ideal space can then be performed for the purpose of correlating the initial candidate object points with points in the ideal space. This computer search (i.e., the satellite correlation analysis) is described in terms of fifteen steps in Table 9. The maximums of the correlation output arrays X, Y, Z and W defined in step 12 provide a direct way of locating the highest correlation between initial candidate objects. In step 15, further examination of candidate objects producing these correlations allows us to verify if any of these correlations correspond to real satellites.

Viking 1 Correlational Analysis

The satellite correlation analysis described in Table 9 was first applied to the Viking 1 approach pictures, since these pictures are significantly more sensitive and less noisy than the Viking 2 approach

pictures. Before applying the correlation analysis, 14 initial candidate objects were eliminated from the list. Five of these objects [number 2, 7, 42, 49 and 52] were identified as camera blemishes that were not in the blemish filter (see Figure 2) and nine objects [number 17, 18, 19, 20, 21, 32, 36, 38 and 39] were then recognized as strong bit errors due to their high DN level above background. The correlation analysis was divided into suitable radial regions. For prograde orbits, results for the A array are shown in the two-dimensional (rectangular) ideal space in Figure 6. The horizontal scale (sample) is the longitude angle about Mars in 0.5 degree increments and the vertical scale (line) is the radial distance from the center of Mars and ranges from 8001 to 10,000 km (from top to bottom) in 3 km increments. The values in the A array are displayed in DN brightness levels, where the brightest possible value is 255 and dark is zero.

In Figure 6, there are ten long needle-like patterns displayed on the ideal space (R,Θ) plane which actually correspond to the eleven initial candidate objects that occur in the radial interval about Mars from 8000 to 10,000 km. The transparent overlay identifies each long needle-like pattern with the object number of its initial candidate object given in Table 6 and furthermore shows us that the long needle-like patterns for object numbers 43 and 46 coincide and therefore appear to have a single signature. Note that from Table 8, there are actually 14 initial candidate objects in Table 6 that are in this radial interval, but three of these objects (numbers 7, 19 and 32) were previously eliminated as blemishes or bit errors (see the discussion above) and were thus not included in the correlation analysis.

Each needle-like pattern is an error ellipse in the ideal space for one of the initial candidate objects. Each error ellipse is formed by displaying only the 30 top brightness levels of the A array (i.e., values between 255 and 225 DN). Since this DN level actually represents a displacement from the candidate object in the image plane (object space), the error ellipses in Figure 6 represent the possible location of each of the 11 initial candidate points in the ideal space for a measurement uncertainly of 30 pixels in location of each initial candidate object in their approach picture. The major measurement

uncertainty is introduced in determining the planet center and was below the 30 pixel error adopted here. Object numbers 3, 5, 10, 14 and 15, which are properly ordered in event time and all occur before the ideal space reference time t_o, have negative slopes (as viewed from the bottom of Figure 6). These objects had to be advanced in time and the more the objects were advanced in time, the smaller the negative slope. Object numbers 27, 34, 43, 46, 48 and 54, which are properly ordered in event time and occur after the ideal space reference time t_o, have positive slopes. These objects had to be backed-up in time and the larger the backup time the smaller the slope. Object 43 and 46 have essentially the same slopes since their event times differ only by about 10 seconds (see Table 6 and then Table 1).

When two or more error ellipses intersect, this indicates that these objects have a high probability of being the same object (i.e., a satellite). Further examination (step 15 of Table 9) is then required to more exactly classify the nature of the correlated maximums. In Figure 6, object numbers 3, 15, 43 and 46 all intersect at a common point. The only other intersection occurs between object number 46 and 10. A closeup of these two interaction points is shown in Figure 7 where brightness contour levels of 245, 235 and 225 DN (i.e., measurement uncertainties of 10, 20 and 30 pixels) have also been shown. Careful examination of the pixel signatures of these initial candidate objects shows that object numbers 3, 15, 43 and 46 are several pixels in size and that the brightness of the object is consistent with the relative camera sensitivity (see Table 6, Table 1 and then Table 5) and spacecraft range. Object number 10 is two pixel in size with pixel brightness values of 60 and 62 and are hence rather discontinuous with the 50 DN background level. This pixel signature is that of a bit error and not a real object imaged by the camera. The intersection of object 10 and 46 is thus of no significance.

In Figure 8, the results of the Z-array (see Table 9, step 12) are displayed for the intersection point of the object numbers 3, 15, 43 and 46, and contour levels similar to Figure 7 are also shown. The maximum of the Z-array indicates that the object must be located on a circular orbit having a radius of 9374 kilometers. This object is the satellite Phobos which has an orbital radius between 9376 and 9377 kilometers.

A comparison of the four detections of Phobos with other approach pictures taken in the same time sequences, but with different camera parameters, is given in Table 10. Phobos was detected in addition in the picture number 169C65 having a 6-pixel signature with 5 pixels having a value of 50 DN and 1 pixel having a value of 52 DN above a background of 48 DN (a signature not strong enough to trip the object locater in Figure 2). In the time sequence 15, the picture numbers 170C31 and 170C33 had a different field of view (than 170C30 and 170C32) that excluded Phobos. Transforming in time and space Phobos into all other picture numbers results in either Phobos being out of the field of view or too far from the spacecraft to produce a detectable signal. The Viking 1 detection results of Phobos summarized in Table 10 also indicate that all the Viking 2 approach pictures (see Table 5) except one [i.e., 219D25 taken in the high gain state that effectively doubles the exposure time] will be below the sensitivity level required to image Phobos.

The correlation analysis was applied to all the Viking 1 initial candidate object data between 4000 and 20,000 kilometer radius. In addition to the results for the radial interval 8000 to 10,000 km discussed above, three other correlation maximums involving two initial candidate objects per correlation were also obtained. The first correlation was between object numbers 9 and 47 having a circular orbit of 4967.5 kilometers radius. Object 47 was subsequently shown to be a camera blemish and object 7 was not present in the more sensitive approach picture 169C47. The second correlation was between object numbers 13 and 25 having an orbital radius of 6665 kilometers. Object 13 and object 25 were not present, respectively, in the more sensitive approach pictures (169C47, 169C51) and (170C15) so that the correlation does not represent a real object. The third correlation was between object numbers 8 and 23 having a circular orbit of 10,881 kilometers radius. Object 23 is not present in the more sensitive approach pictures 170C08 and 170C12 and furthermore, it is a bit error so that the correlation does not represent a real object.

A retrograde correlational analysis was then applied to all the Viking 1 initial candidate points. Three correlation maximums were obtained. The first correlation was between object number 9 and 37

having a circular orbit of 5220 kilometer radius. Both objects were subsequently recognized as bit errors. The second correlation was between three Phobos objects with object number 3, 43 and 46 giving an incorrect orbital radius of 9156 kilometers. Object 43 and 46 are only about 10 seconds apart in event time so that they easily fit in a retrograde orbit. The third correlation was between object number 10 and 27 having an orbital radius of 9528 kilometers. Object 10 is a bit error and object 27 is not present in the more sensitive time sequence approach picture 170C15. The retrograde analysis therefore provided no new satellite objects.

After performing the prograde and retrograde correlational analysis, the pixel signatures of all the 54 candidates were carefully studied and intercompared. Additional camera blemishes and bit errors were identified and classified. All objects larger than two pixels, except Phobos, were identified as camera blemishes. All remaining two-pixel objects which had a pixel signature larger than 10 DN above background were seen to be bit errors. In the Viking 1 initial candidate list of 54 objects there are 18 camera blemishes, 19 bit errors and 4 detections of Phobos, leaving 13 unidentified two pixel objects having brightness signatures no greater than 10 DN above background (see Table 6). Because of the inability to identify object numbers 11, 12 and 14 in the more sensitive time-sequence approach picture 160C47, the object numbers 22 and 24 in the more sensitive picture 170C08, the object numbers 25 and 27 in the more sensitive picture 170C15, object number 33 in the more sensitive picture 170C29, object number 50 in the more sensitive picture 170C36 and finally object number 51 in the more sensitive picture 170C37, the Viking 1 initial candidate list can be reduced to only three unidentified objects [numbers 6, 8 and 16]. The two pixel signature of object 6 (54 and 60 DN above a 50DN background) is almost certainly a bit error. The two-pixel signatures of object numbers 8 and 16 are only 4 DN above the background level and are likely random bit errors of low DN values but cannot be further differentiated from a satellite object having a signal just above the background.

Viking 2 Correlational Analysis

Because of the low values of the relative sensitivity and the much higher noise levels of the Viking 2 approach pictures in comparison to those for the Viking 1 approach pictures and the inability to detect any new satellite in the Viking 1 approach pictures, a complete correlational analysis for the Viking 2 approach pictures was not performed. A limited analysis was, however, applied for prograde orbits to the candidate objects that project into the equatorial plane in the radial interval between 8,000 and 10,000 km. This radial interval was chosen because it includes the orbital radius of Phobos (9376-9377 km). Using the location of Phobos in the Viking 1 approach picture set, the predicted locations of Phobos in all Viking 2 approach pictures were calculated and compared to location of the Viking 2 initial candidate objects. Only object number 200 in picture number 219D25 compared favorably with the predicted location. Picture number 219D25 has the highest relative sensitivity of all pictures in the Viking 2 approach pictures (see Table 5) because it was taken with a high gain camera setting (see Table 2) which doubles the camera sensitivity compared to the low gain camera setting. Object number 200 may well be a detection of Phobos, but it cannot be confirmed by the remaining less sensitive Viking 2 approach pictures.

The general correlation analysis was then applied to all Viking 2 initial candidate objects in the 8000 to 10,000 km radial interval. Five correlations involving more than two initial candidate objects were present in addition to a number of correlations involving only two initial candidate objects. Only the five correlations that involved more than two initial candidate objects were examined. The first of these correlations was for an orbital radius of 8040 km and involved object numbers 50, 229 and 247. Objects 229 and 247 do not appear in the more sensitive picture number 219D26 of the same time sequence so that the correlation does not represent a real object. The second correlation, at an orbital radius of 8163 for object numbers 171, 173, 229 and 247, is also not real for the same reason since object number 171 does not occur in picture number 219D02 and both object numbers 229 and 247 are absent in picture number 219D26. The third

correlation, at an orbital radius of 8268 for object numbers 30, 38, 282 and 337, is also not real. Ojbect number 282 is a camera blemish and the pixel size and brightness of object numbers 337, 38 and 30 are not consistent when the spacecraft distance from Mars is considered. The fourth correlation, at an orbital radius of 8771 km for object numbers 104, 316 and 324, does not represent a real object since object numbers 316 and 324 are not present in the more sensitive picture number 219D54. The fifth correlation, at an orbital radius of 8915 km for object numbers 141, 183 and 350, is not of a real object since object numbers 183 and 350 are respectively not in the more sensitive picture numbers 219D10 and 219D64.

The final investigation of initial candidate objects in Table 7 was to examine closely all objects larger than two pixels in size. This exercise led to the discovery of many new camera blemishes not originally contained in the blemish filter (see Figure 2), to an object that was on the planet disc, to an object that was a camera reseau, to objects that were bit errors, and finally to objects that were random errors (i.e., not visible in a more sensitive picture number exposed in the same time sequence). Only object number 278 which is three pixels in size, remains as a qualified object larger than two pixels in size. This object occurs in picture number 219D44 which is the most sensitive picture in this time sequence and therefore cannot be disqualified. This object is likely a random error but study of its pixel signature is not conclusive because it is only 4 DN above the background level. All two-pixel objects in Table 7 were not analyzed beyond their classification of brightness above background.

IV. CONCLUDING REMARKS

Data analysis of the Viking 1 and Viking 2 approach pictures to search for new satellites of Mars has been performed using new software tools that were created at the Image Processing Laboratory at JPL especially for this project. The search procedure resulted in no new satellites. The quality of the Viking 1 approach pictures was sufficient to detect objects having similar size and brightness as Phobos. Phobos was detected five times in the Viking 1 approach pictures and possibly once in the Viking 2 approach pictures. The exposure times for the Viking 1 approach pictures were chosen to properly image Mars and were significantly shorter than the maximum exposure times that would have optimized the camera for detection of new satellites. The quality of the Viking 2 approach pictures was significantly poorer than the Viking 1 approach pictures because of shorter exposure times, inferior transmission of the color filters, and noisier background characteristics of the cameras. This made the Viking 2 approach pictures essentially useless for detecting new satellites of Mars.

Data analysis of the Viking 1 approach pictures was divided into three stages: (1) screening of the image data to obtain an initial list of possible candidate objects, (2) navigation processing of the candidate object data, and (3) correlation analysis of the candidate objects. The first two stages of the data analysis provided a list of 54 initial candidate objects (Table 6) which were analyzed in detail in stage 3. Four of these objects were determined to be Phobos. Of the 50 remaining objects, 18 objects were camera blemishes and 19 objects were bit errors, and 10 objects were identified as random errors, leaving only three unidentified objects (object numbers 6, 8 and 16 of Table 6). Of these three objects, object number 6 is almost certainly a bit error and the other two objects are likely random bit errors of low DN values which cannot further be differentiated from a satellite object having a signal just above the background brightness level of the image.

From the analysis of the Viking 1 and Viking 2 approach pictures, it must be concluded that no new satellites of Mars have been discovered. This finding is consistent with the results of Duxbury (1983) who, in a parallel search effort to discover new satellites of Mars, used pictures taken by the Viking Orbiter late in its mission. These pictures were taken with the Viking Orbiter in the equatorial plane of Mars and viewed the area within one degree of the equatorial plane and radially from the limb of Mars to the orbit of Phobos. Three sequences of pictures were taken separated by 30 minutes and covered the equatorial viewing area on both sides of Mars. Analysis of these pictures by Duxbury allowed him to conclude that no satellite with a diameter of 200 km (or larger) and having a similar albedo to Phobos or Deimos were present in his time-space viewing area. The Viking approach pictures were much less sensitive but had a superior time window in comparison to the Viking Orbiter pictures. The two search procedures thus had somewhat complementary data sets.

Acknowledgement

The high quality of work, thorough effort and the creative development of software tools for this satellite search project can be credited in large measure to the excellence and tireless efforts of Gary Yagi of the Image Processing Laboratory. The author is greatly appreciative of Gary's full and unwavering support throughout this long and rather tedious project.

REFERENCES

Duxbury, T.C. (1983) Private communication.

French, R.G. and Elliot, J.L. (1979) Occultation of ε Geminorus by Mars. III. Temperature Structure of the Martian Upper Atmosphere. Ap. J., 229, 828.

French, R.G., Goguen, J.D. and Duthie, J.G. (1978) Martian Occultation of ε Gem as Observed from the C.E. Kenneth Mees Observatory. Icarus, 34, 182.

Liller, W., Papaliolios, C., French, R.G., Elliot, J.L. and Church, C. (1978) The Occultation of ε Gem by Mars as Observed from Agassiz Station. Icarus, 35, 395.

McCook, G.P. (1979) Private communication.

Table 1. Viking 1 Approach Picture Information

Time Sequence	Pic. No.	Picture Inf.		Camera				Spacecraft: Loc/Time				
		Quality	View	A/B	Exp (ms)	Gain	Filter	RMAG (km)	Event DDD	HH	MM	S
1	169C01	Noisy		A	407.3	low	VLT	680,278	169	01	02	50.177
	169C02	smear		B	135.8	low	RED	680,266	169	01	02	54.521
2	169C03			A	135.8	low	VLT	641,367	169	05	08	56.263
	169C04	Blank		B	0.00	low	BLU	641,356	169	05	09	00.607
3	169C05			A	407.3	low	VLT	628,471	169	06	30	28.424
	169C09			A	67.88	low	GRN	628,424	169	06	30	46.174
	169C11			A	135.8	low	RED	628,400	169	06	30	55.168
4	169C19			A	407.3	low	VLT	583,004	169	11	17	47.471
	169C23			A	67.88	low	GRN	582,957	169	11	18	05.221
	169C25			A	135.8	low	RED	582,934	169	11	18	14.215
5	169C26			A	407.3	low	VLT	563,591	169	13	20	23.634
	169C30			A	67.88	low	GRN	563,545	169	13	20	41.384
	169C32			A	135.8	low	RED	563,521	169	13	20	50.378
6	169C33			A	407.3	low	VLT	544,124	169	15	23	17.717
	169C37			A	67.88	low	GRN	544,077	169	15	23	35.467
	169C39			A	135.8	low	RED	544,054	169	15	23	44.461
7	169C40	Blank		A	0.00	low	VLT	524.625	169	17	26	20.760
	169C44	Blank		A	0.00	low	VLT	524,579	169	17	26	38.510
	169C46	Blank		A	0.00	low	VLT	524,555	169	17	26	47.504
8	169C47			A	407.3	low	RED	505,118	169	19	29	23.803
	169C51			A	67.88	low	MBL	505,071	169	19	29	41.553
	169C53			A	135.8	low	VLT	505,047	169	19	29	50.547
9	169C61			A	407.3	low	VLT	466,265	169	23	34	18.209
	169C65			A	67.88	low	GRN	466,218	169	23	34	35.959
	169C67			A	135.8	low	RED	466,195	169	23	34	44.953
10	170C01			A	407.3	low	VLT	446,729	170	01	37	21.252
	170C05			A	67.88	low	GRN	446,682	170	01	37	39.002
	170C07			A	135.8	low	RED	446,658	170	01	37	47.996
11	170C08			A	407.3	low	VLT	427,180	170	03	40	24.294
	170C12			A	67.88	low	GRN	427,133	170	03	40	42.044
	170C14			A	135.8	low	RED	427,110	170	03	40	51.038
12	170C15			A	203.6	low	VLT	407,691	170	05	43	00.457
	170C19			A	67.88	low	GRN	407,644	170	05	43	18.207
	170C21			A	135.8	low	RED	407,620	170	05	43	27.201
13	170C22			A	203.6	low	VLT	388,592	170	07	43	04.300
	170C23			A	67.88	low	GRN	388,545	170	07	43	22.050
	170C25			A	135.8	low	RED	388,521	170	07	43	31.044
14	170C26			A	50.91	low	MBL	368,235	170	09	51	02.929
	170C27			B	50.91	low	MBL	368,207	170	09	51	07.324
	170C28			A	407.3	low	VLT	368,194	170	09	51	11.983
	170C29			B	407.3	low	VLT	368,183	170	09	51	16.463

Table 1 (Continued)

Time Sequence	Pic. No.	Picture Inf.		Camera				Spacecraft: Loc/Time	
		Quality	View	A/B	Exp (ms)	Gain	Filter	Rmag (km)	Event DDD HH MM S
15	170C30			A	50.91	low	MBL	348,628	170 11 54 05.971
	170C31			B	50.91	low	MBL	348,616	170 11 54 10.451
	170C32			A	407.3	low	VLT	348,604	170 11 54 15.111
	170C33			B	407.3	low	VLT	348,592	170 11 54 19.590
16	170C34			A	50.91	low	MBL	329,011	170 13 56 59.970
	170C35			B	50.91	low	MBL	329,000	170 13 57 04.450
	170C36			A	407.3	low	VLT	329,987	170 13 57 09.109
	170C37			B	407.3	low	VLT	328,975	170 13 57 13.589
17	170C38			A	203.6	low	VLT	309,366	170 16 00 03.192
	170C39	smear		B	135.8	low	RED	309,354	170 16 00 07.536
	170C40	smear		A	407.3	low	VLT	309,342	170 16 00 12.152
	170C41	smear		B	135.8	low	RED	309,330	170 16 00 16.496
18	170C42			A	203.6	low	VLT	289,697	170 18 03 06.235
	170C43	smear		B	135.8	low	RED	289,685	170 18 03 10.579
	170C44	smear		A	407.3	low	VLT	289,673	170 18 03 15.195
	170C45	smear		B	135.8	low	RED	289,661	170 18 03 19.539
19	170C46			A	203.6	low	VLT	270,026	170 20 06 00.318
	170C47	smear		B	135.8	low	RED	270,014	170 20 06 04.662
	170C48	smear		A	407.3	low	VLT	270,002	170 20 06 09.278
	170C49	smear		B	135.8	low	RED	269,990	170 20 06 13.622

Table 2. Viking 2 Approach Picture Information

Time Sequence	Pic. No.	Picture Inf.		Camera				Spacecraft: Loc/Time	
		Quality	View	A/B	Exp (ms)	Gain	Filter	Rmag (km)	Event DDD HH MM S
1	218D01			A	203.6	low	VLT	579,221	218 01 04 06.17
	218D02			B	67.88	low	RED	579,210	218 01 04 10.58
2	218D03			A	203.6	low	VLT	559,588	218 03 07 00.25
	218D04			B	67.88	low	RED	559,576	219 03 07 04.66
3	218D05			A	203.6	low	VLT	539,923	218 05 10 03.29
	218D06			B	67.88	low	RED	539,911	218 05 10 07.70
4	218D08			B	203.6	low	VLT	520,238	218 07 13 10.81
	218D12			B	50.91	low	GRN	520,190	218 07 13 28.66
	218D14			B	67.88	low	RED	520,166	218 07 13 37.63
5	218D16			B	203.6	low	VLT	500,580	218 09 16 14.90
	218D20			B	50.91	low	GRN	500,531	218 09 16 23.199
	218D22	noisy		B	67.88	low	RED	500,507	218 09 16 32.168
6	218D24			B	203.6	low	VLT	480,884	218 11 19 07.94
	218D28			B	50.91	low	GRN	480,842	218 11 19 25.78
	218D30			B	67.88	low	RED	480,817	218 11 19 34.75
7	218D48			B	203.6	low	VLT	421.608	218 17 29 11 283
	218D52			B	50.91	low	GRN	421,561	218 17 29 29.127
	218D54			B	67.88	low	RED	421,537	218 17 29 38.096
8	218D56			B	203.6	low	VLT	401,896	218 19 32 05.366
	218D60			B	50.91	low	GRN	401,848	218 19 32 23.209
	218D62			B	67.88	low	RED	401,824	218 19 32 32.178
9	218D64			B	203.6	low	VLT	382,146	218 21 35 08.407
	218D68			B	50.91	low	GRN	382,098	218 21 35 26.220
	218D70			B	67.88	low	RED	382,074	218 21 35 35.220
10	218D72			B	203.6	low	VLT	362,404	218 23 38 02.489
	218D76			B	50.91	low	GRN	362,356	218 23 38 20.333
	218D78			B	67.88	low	RED	362,332	218 23 38 29.302
11	219D02			B	203.6	low	VLT	342,621	219 01 41 05.532
	219D06			B	50.91	low	GRN	342,573	219 01 41 23.375
	219D08			B	67.88	low	RED	342,549	219 01 41 32.344
12	219D10			B	203.6	low	VLT	322,818	219 03 44 08.574
	219D14			B	50.91	low	GRN	322,770	219 03 44 26.418
	219D16			B	67.88	low	RED	322,746	219 03 44 35.366
13	219D18			B	203.6	low	VLT	303,018	219 05 47 02.656
	219D22			B	50.91	low	GRN	302,970	219 05 47 20.500
	219D24	missing		B	67.88	low	RED	302,948	219 05 47 29.016
14	219D25	noisy		A	203.6	high	VLT	283,183	219 07 50 00.766
	219D26	noisy		B	203.6	low	VLT	283,171	219 07 50 05.246
	219D29			A	33.94	low	GRN	283,135	219 07 50 18.601
	219D30			B	50.91	low	GRN	283,123	219 07 50 23.089
	219D31			A	67.88	low	RED	283,111	219 07 50 27.578
	219D32			B	67.88	low	RED	288,099	219 07 50 32.058

Table 2 (Continued)

Time Sequence	Pic. No.	Picture Inf.		Camera				Spacecraft: Loc/Time	
		Quality	View	A/B	Exp (ms)	Gain	Filter	Rmag (km)	Event DDD HH MM S
15	219D33			A	203.6	low	VLT	263,307	219 09 53 03.809
	219D34			B	203.6	low	VLT	263,295	219 09 53 08.269
	219D37			A	33.94	low	GRN	263,259	219 09 53 21.644
	219D38			B	50.91	low	GRN	263,247	219 09 53 26.132
	219D39			A	67.88	low	RED	263,235	219 09 53 30.621
	219D40			B	67.88	low	RED	263,223	219 09 53 35.101
16	219D43			A	203.6	low	VLT	243,423	219 11 55 57.891
	219D44			B	203.6	low	VLT	243,411	219 11 56 02.371
	219D47			A	33.94	low	GRN	243,375	219 11 56 15.726
	219D48			B	50.91	low	GRN	243,362	219 11 56 20.666
	219D49			A	67.88	low	RED	243,350	219 11 56 25.155
	219D50			B	67.88	low	RED	243,338	219 11 56 29.634
17	219D53			A	203.6	low	VLT	223,477	219 13 59 01.384
	219D54			B	203.6	low	VLT	223,465	219 13 59 05.864
	219D57			A	33.94	low	GRN	223,430	219 13 59 18.768
	219D58			B	50.91	low	GRN	223,418	219 13 59 23.256
	219D59			A	67.88	low	RED	223,405	219 13 59 27.745
	219D60			B	67.88	low	RED	223,393	219 13 59 32.225
18	219D63			A	203.6	low	VLT	203,488	219 16 02 03.976
	219D64			B	203.6	low	VLT	203,476	219 16 02 08.456
	219D67			A	33.94	low	GRN	203,440	219 16 02 21.811
	219D68			B	50.91	low	GRN	203,428	219 16 02 26.299
	219D69			A	67.88	low	RED	203,416	219 16 02 30.788
	219D70	missing		B	67.88	low	RED	203,404	219 16 02 35.268

Table 3. Camera Spatial Resolution and Phobos Imaging

Spacecraft Distance to Mars (km)	Apparent Pixel Size (km)	Phobos Image Plane Size (pixel)	Phobos Brightness (magnitudes)
800,000	20.0	1.0	1.55
700,000	17.5	1.1	1.26
600,000	15.0	1.3	0.92
500,000	12.5	1.6	0.53
400,000	10.0	2.0	0.42
300,000	7.5	2.7	-0.58
200,000	5.0	4.0	-1.46

Table 4. Absolute Sensitivity† of the Viking 1 and Viking 2 Cameras

Filter Color	Viking 1 Camera A (DN/ms)	Viking 1 Camera B (DN/ms)	Viking 2 Camera A (DN/ms)	Viking 2 Camera B (DN/ms)
Blue	9.01	8.88	9.98	7.98
Minus Blue	17.84	14.62	17.74	15.35
Violet	4.95	3.82	3.54	4.06
Clear	26.47	22.59	25.07	22.95
Green	13.51	11.23	13.24	11.66
Red	5.00	4.14	5.06	4.42

†These are camera filter factors determined for the low gain state for solar irradiance at 1.63AU given in the Viking Flight Memorandum OIT-21334-KK (September 21, 1977)

Table 5. Approach Pictures: Summary of the Number of Exposures and their Relative Sensitivity†

Filter Color	Exposure Time (ms)	Viking 1				Viking 2			
		Camera A		Camera B		Camera A		Camera B	
		Number	Sensitivity	Number	Sensitivity	Number	Sensitivity	Number	Sensitivity
Violet	407.3	14	2.02	3	1.56	(1)	1.44	-	-
	203.6	5	1.01	-	-	7	0.72	15	0.83
	135.8	2	0.67	-	-	-	-	-	-
Minus Blue	67.88	1	1.21	-	-	-	-	-	-
	50.91	3	0.91	3	0.74	-	-	-	-
Green	67.88	9	0.92	-	-	-	-	-	-
	50.91	-	-	-	-	-	-	15	0.59
	33.94	-	-	-	-	5	0.45	-	-
Red	407.3	1	2.04	-	-	-	-	-	-
	135.8	9	0.68	7	0.56	-	-	-	-
	67.88	-	-	-	-	5	0.34	18	0.30
		44		13		18		48	

†Relative Sensitivity (10^3DN) = (Exposure Time)(Filter Factor of Table 4).

Table 6: Viking 1 Approach Pictures: Initial Candidate Object List

Object Number	Picture Number	Object Coordinates (L,S)	Object Size (pixel)	Camera Blemishes and Local Maximums	Object Background (DN)	Object Brightness above Background (DN) (1-10)	(11-20)	(21-30)	(>30)
1	169C05	(1094,1133)	6	Blemish	-	-	-	-	-
2	169C23	(896, 107)	2	Blemish	-	-	-	-	-
3	169C26	(234, 276)	4	-	48-50	4	-	-	-
4	169C39	(736,1127)	2	Blemish	-	-	-	-	-
5	169C47	(308,1099)	2	-	46-48	-	12	-	-
6	169C47	(564, 894)	2	-	48-50	10	-	-	-
7	169C47	(896, 108)	2	Blemish	-	-	-	-	-
8	169C47	(929, 740)	2	-	48-50	4	-	-	-
9	169C51	(89, 901)	2	-	44-46	-	12	-	-
10	169C51	(502, 45)	2	-	50	-	12	-	-
11	169C51	(547, 335)	2	-	50-52	6	-	-	-
12	169C51	(705, 172)	2	-	50-52	6	-	-	-
13	169C53	(228,1024)	2	-	46-48	-	-	22	-
14	169C53	(830, 755)	2	-	48-50	10	-	-	-
15	169C61	(260,1079)	4	-	48	8	-	-	-
16	169C61	(479, 950)	2	-	48-50	4	-	-	-
17	169C67	(911, 199)	2	-	48-50	-	-	-	130
18	170C05	(321,1139)	2	-	48	-	-	-	130
19	170C08	(894, 926)	2	-	48	-	-	-	96
20	170C12	(134, 479)	2	-	46	-	-	-	194
21	170C12	(284, 391)	2	-	48	-	-	-	184
22	170C14	(391, 848)	2	-	46-48	10	-	-	-
23	170C14	(658,1106)	2	-	48	-	-	-	32
24	170C14	(1061,1195)	2	-	50-52	4	-	-	-
25	170C19	(858, 512)	2	-	48-50	10	-	-	-
26	170C19	(859, 947)	2	-	48	-	16	-	-
27	170C19	(1013, 623)	2	-	48-50	4	-	-	-
28	170C19	(1076,1218)	2	Blemish		-	-	-	-
29	170C27	(354, 372)	2	Blemish		-	-	-	-
30	170C27	(552, 246)	2	Blemish		-	-	-	-

Table 6 (continued)

Object Number	Picture Number	Object Coordinates (L,S)	Object Size (pixel)	Camera Blemishes and Local Maximums	Object Background (DN)	Object Brightness above Background (DN) (1-10)	(11-20)	(21-30)	(>30)
31	170C27	(775,1087)	2	-	36	-	-	-	38
32	170C27	(879, 271)	2	-	34	-	-	-	152
33	170C27	(830,1011)	2	-	34-36	4	-	-	-
34	170C27	(954, 225)	2	Blemish	-	-	-	-	-
35	170C27	(1087, 419)	3	Blemish	-	-	-	-	-
36	170C28	(872, 476)	2	-	50	-	-	-	160
37	170C28	(891, 361)	2	-	50-52	-	16	-	-
38	170C28	(924, 916)	2	-	50	-	-	-	192
39	170C28	(973, 455)	2	-	50	-	-	-	64
40	170C29	(95,1090)	2	-	32-34	-	16	-	-
41	170C29	(661, 535)	2	Blemish	-	-	-	-	-
42	170C29	(820, 882)	2	Blemish	-	-	-	-	-
43	170C30	(155, 388)	3-15	-	48	4	-	-	-
44	170C31	(1016,1206)	4	Blemish	-	-	-	-	-
45	170C31	(1057, 440)	3	Blemish	-	-	-	-	-
46	170C32	(136, 406)	6-8	-	50	8	-	-	-
47	170C32	(597, 576)	2	Blemish	-	-	-	-	-
48	170C33	(661, 535)	2	Blemish	-	-	-	-	-
49	170C33	(820, 882)	2	Blemish	-	-	-	-	-
50	170C34	(79, 915)	2	-	46-48	4	-	-	-
51	170C35	(739, 856)	2	-	34-36	4	-	-	-
52	170C35	(820, 882)	2	Blemish	-	-	-	-	-
53	170C36	(127, 75)	2		46-48	-	-	-	96
54	170C42	(736,1126)	4	Blemish	-	-	-	-	-

Table 7: Viking 2 Approach Pictures: Initial Candidate Object List

Object Number	Pictures Number	Object Coordinates (L,S)	Object Size (pixel)	Camera Blemishes and Local Maximums	Object Background (DN)	Object Brightness above Background (DN) (1-10)	(11-20)	(21-30)	(<30)
1	218D01	(407, 245)	2	-	40	6	-	-	-
2	218D01	(837, 917)	2	Blemish	-	-	-	-	-
3	218D01	(968, 215)	2	-	40	6	-	-	-
4	218D01	(972, 497)	2	-	38	10	-	-	-
5	218D01	(1103,1101)	2	-	42	4	-	-	-
6	218D02	(718, 677)	2	-	42-44	-	16	-	-
7	218D02	(757, 796)	2	-	42	4	-	-	-
8	218D02	(847, 108)	2	-	54	4	-	-	-
9	218D02	(872, 897)	2	-	44-46	-	16	-	-
10	218D02	(882,1044)	2	-	48	10	-	-	-
11	218D02	(1070, 240)	2	-	50-52	6	-	-	-
12	218D02	(1068,1081)	2	-	48-50	4	-	-	-
13	218D03	(78, 865)	2	-	50	4	-	-	-
14	218D03	(347,1020)	2	-	48	10	-	-	-
15	218D03	(523, 529)	2	Blemish	-	-	-	-	-
16	218D03	(691, 53)	3	Blemish	-	-	-	-	-
17	218D03	(687, 901)	5	Blemish	-	-	-	-	-
18	218D03	(770, 940)	2	-	42-44	4	-	-	-
19	218D03	(918, 216)	2	-	40	-	18	-	-
20	218D04	(172, 547)	2	-	48-50	-	-	-	38
21	218D04	(227, 733)	2	-	46	-	-	30	-
22	218D04	(500, 55)	2	-	58	4	-	-	-
23	218D04	(613, 852)	2	-	42	8	-	-	-
24	218D04	(828,1086)	2	-	46-48	6	-	-	-
25	218D04	(920, 811)	2	-	46	-	12	-	-
26	218D04	(928, 406)	2	-	46-48	4	-	-	-
27	218D04	(936,1016)	2	-	46-48	4	-	-	-
28	218D04	(1062, 890)	2	-	46-48	8	-	-	-
29	218D04	(1062, 897)	2	-	46-48	-	-	-	32
30	218D04	(1102, 415)	2	-	48-50	4	-	-	-

Table 7 (Continued)

Object Number	Pictures Number	Object Coordinates (L,S)	Object Size (pixel)	Camera Blemishes and Local Maximums	Object Background (DN)	Object Brightness above Background (DN) (1-10)	(11-20)	(21-30)	(<30)
31	218D05	(192, 677)	2	-	48	-	16	-	-
32	218D05	(404, 615)	2	-	44	-	12	-	-
33	218D05	(422, 802)	2	-	44-46	4	-	-	-
34	218D05	(551,1218)	6	Blemish	-	-	-	-	-
35	218D05	(893, 544)	2	-	38-40	6	-	-	-
36	218D05	(1076, 960)	2	-	42	4	-	-	-
37	218D06	(181, 281)	2	-	52	-	-	-	32
38	218D06	(247, 175)	2	-	54	4	-	-	-
39	218D06	(292, 370)	2	-	48-50	4	-	-	-
40	218D06	(397, 339)	2	(on Mars disc)	48-50	4	-	-	-
41	218D06	(400, 346)	3	(on Mars disc)	48	4	-	-	-
42	218D06	(432, 248)	2	-	48	-	-	-	36
43	218D06	(422,1160)	4	Blemish	-	-	-	-	-
44	218D06	(454, 572)	2	-	42-44	-	-	-	40
45	218D06	(1011, 39)	2	-	54-56	4	-	-	-
46	218D06	(1013, 373)	2	-	48	10	-	-	-
47	218D08	(197, 100)	2	-	56-58	4	-	-	-
48	218D08	(365, 80)	3	Blemish	-	-	-	-	-
49	218D08	(481, 759)	2	-	42-44	4	-	-	-
50	218D08	(764, 356)	2	-	42	4	-	-	-
51	218D08	(948, 425)	2	-	46-48	4	-	-	-
52	218D08	(1109,1130)	2	-	48-50	4	-	-	-
53	218D12	(132, 50)	2	-	58-60	4	-	-	-
54	218D12	(147, 434)	2	-	50-52	4	-	-	-
55	218D12	(282, 47)	2	-	58-60	4	-	-	-
56	218D12	(855,1045)	2	-	46	4	-	-	-
57	218D12	(1083,1007)	2	-	48	4	-	-	-
58	218D14	(380, 264)	2	-	50-52	4	-	-	-
59	218D14	(527, 41)	2	-	58-60	4	-	-	-
60	218D14	(1029, 95)	2	-	54-56	4	-	-	-

Table 7 (Continued)

Object Number	Pictures Number	Object Coordinates (L,S)	Object Size (pixel)	Camera Blemishes and Local Maximums	Object Background (DN)	Object Brightness above Background (DN) (1-10)	(11-20)	(21-30)	(<30)
61	218D16	(82, 819)	2	-	52-54	4	-	-	-
62	218D16	(115, 104)	2	-	58	4	-	-	-
63	218D16	(366, 836)	2	-	44-46	4	-	-	-
64	218D16	(415, 100)	2	-	58	4	-	-	-
65	218D16	(567, 221)	2	-	52-54	4	-	-	-
66	218D16	(764, 374)	2-5	Blemish	-	-	-	-	-
67	218D16	(1078, 260)	2	-	52	4	-	-	-
68	218D20	(156, 489)	2	-	50	-	-	-	32
69	218D20	(166,1099)	2	-	50-52	4	-	-	-
70	218D20	(260, 42'	2	-	58-60	4	-	-	-
71	218D20	(256, 85(	2	-	46	8	-	-	-
72	218D20	(650, 15/	2	-	54-56	4	-	-	-
73	218D20	(840, 39)	2	-	58-60	4	-	-	-
74	218D20	(858, 104)	2	-	56-58	4	-	-	-
75	218D20	(898, 273)	3	Blemish	-	-	-	-	-
76	218D20	(1059,1066)	2	-	50-52	-	14	-	-
77	218D24	(901, 178)	2	Blemish	-	-	-	-	-
78	218D24	(1072, 940)	2	Reseau	-	-	-	-	-
79	218D28	(98, 99)	2	-	58-60	4	-	-	-
80	218D28	(117, 356)	2	-	52-54	4	-	-	-
81	218D28	(247, 481)	2	-	48	4	-	-	-
82	218D28	(338, 88)	2	-	58-60	4	-	-	-
83	218D28	(569, 252)	2	-	50	4	-	-	-
84	218D28	(1057, 980)	2	-	48	4	-	-	-
85	218D30	(317, 315)	2	-	50-52	4	-	-	-
86	218D30	(398, 466)	2	-	46	4	-	-	-
87	218D30	(448, 174)	2	-	54	4	-	-	-
88	218D30	(689, 233)	2	-	50	4	-	-	-
89	218D30	(728, 71)	2	-	58-60	4	-	-	-
90	218D30	(891, 424)	2	-	46	4	-	-	-

Table 7 (Continued)

Object Number	Pictures Number	Object Coordinates (L,S)	Object Size (pixel)	Camera Blemishes and Local Maximums	Object Background (DN)	Object Brightness above Background (DN) (1-10)	(11-20)	(21-30)	(<30)
91	218D30	(976, 125)	2	-	54	4	-	-	-
92	218D30	(1053,1141)	2	-	50-52	4	-	-	-
93	218D48	(132, 342)	2	-	52	4	-	-	-
94	218D48	(214, 98)	2	-	58-60	4	-	-	-
95	218D48	(216, 51)	2	-	38	-	-	24	-
96	218D48	(354, 173)	2	-	56	4	-	-	-
97	218D48	(389, 273)	2	-	50	-	12	-	-
98	218D48	(590, 410)	2	-	46-48	4	-	-	-
99	218D48	(651, 283)	2	-	50	-	14	-	-
100	218D48	(665, 395)	2	-	46-48	4	-	-	-
101	218D48	(767, 409)	2	-	46	4	-	-	-
102	218D48	(849, 442)	2	-	46	-	-	-	32
103	218D48	(908, 455)	2	-	48	8	-	-	-
104	218D48	(929, 946)	2	-	46	4	-	-	-
105	218D48	(971, 276)	2	-	50-52	4	-	-	-
106	218D48	(1074, 812)	2	-	48	4	-	-	-
107	218D52	(465, 365)	2	-	48-50	4	-	-	-
108	218D52	(475, 176)	2	-	52-54	4	-	-	-
109	218D52	(510, 86)	2	-	58-60	4	-	-	-
110	218D52	(517,1107)	2	-	48	-	-	-	50
111	218D52	(710, 255)	2	Blemish	-	-	-	-	-
112	218D52	(905, 356)	2	-	50-52	4	-	-	-
113	218D52	(1011, 447)	2	-	48-50	4	-	-	-
114	218D52	(1038, 502)	2	-	48-50	4	-	-	-
115	218D52	(1062, 327)	2	-	50-52	4	-	-	-
116	218D52	(1067, 384)	2	-	50-52	4	-	-	-
117	218D52	(1066,1091)	2	-	50	8	-	-	-
118	218D52	(1076, 119)	2	-	54	4	-	-	-
119	218D54	(95, 106)	2	-	58	4	-	-	-
120	218D54	(102, 98)	2	-	58	4	-	-	-

Table 7 (Continued)

Object Number	Pictures Number	Object Coordinates (L,S)	Object Size (pixel)	Camera Blemishes and Local Maximums	Object Background (DN)	Object Brightness above Background (DN) (1-10)	(11-20)	(21-30)	(<30)
121	218D54	(131, 51)	2	-	58-60	4	-	-	-
122	218D54	(138, 322)	2	-	52-54	4	-	-	-
123	218D54	(294, 234)	2	-	52-54	4	-	-	-
124	218D54	(710, 256)	3	Blemish	-	-	-	-	-
125	218D54	(730, 514)	2	-	44	-	-	22	-
126	218D54	(799, 557)	2	-	44-46	4	-	-	-
127	218D54	(879, 51)	2	Blemish	-	-	-	-	-
128	218D56	(306, 155)	2	-	54-56	4	-	-	-
129	218D56	(523, 76)	2	-	58-60	4	-	-	-
130	218D56	(901, 120)	2	-	52-54	4	-	-	-
131	218D60	(118 60)	2	-	58	4	-	-	-
132	218D60	(116, 873)	2	-	50-52	4	-	-	-
133	218D60	(418, 96)	2	-	58-60	4	-	-	-
134	218D60	(456, 352)	2	-	48-50	4	-	-	-
135	218D60	(968, 630)	2	-	46	-	14	-	-
136	218D62	(943,1029)	2	-	48-50	-	14	-	-
137	218D62	(1038,1104)	2	-	50-52	4	-	-	-
138	218D64	(129, 230)	2	-	54	4	-	-	-
139	218D64	(182,1097)	2	-	48-50	4	-	-	-
140	218D64	(192, 914)	2	-	48	4	-	-	-
141	218D64	(614, 379)	2	-	46	4	-	-	-
142	218D64	(765, 520)	2	-	44-46	4	-	-	-
143	218D64	(923,1014)	2	-	48-50	4	-	-	-
144	218D64	(976,1124)	2	-	50-52	4	-	-	-
145	218D68	(85, 578)	2	-	52	4	-	-	-
146	218D68	(573, 44)	3	(Random Error)	-	-	-	-	-
147	218D68	(847, 647)	2	-	44-46	4	-	-	-
148	218D68	(933, 615)	2	-	46	4	-	-	-
149	218D70	(240, 85)	2	-	58	4	-	-	-
150	218D70	(339, 515)	2	-	46-48	4	-	-	-

Table 7 (Continued)

Object Number	Pictures Number	Object Coordinates (L,S)	Object Size (pixel)	Camera Blemishes and Local Maximums	Object Background (DN)	Object Brightness above Background (DN) (1-10)	(11-20)	(21-30)	(<30)
151	218D70	(736, 47)	2	-	58	4	-	-	-
152	218D70	(753, 140)	2	-	54	8	-	-	-
153	218D70	(796, 382)	2	-	46-48	4	-	-	-
154	218D72	(170,1099)	2	-	50	4	-	-	-
155	218D76	(710, 357)	2	-	50-52	4	-	-	-
156	218D76	(885, 84)	2	-	56-58	4	-	-	-
157	218D76	(999, 427)	2	-	48	6	-	-	-
158	218D78	(296,1167)	2	-	48-50	4	-	-	-
159	218D78	(365, 80)	2	Blemish	-	-	-	-	-
160	218D78	(632, 314)	2	-	48	6	-	-	-
161	218D78	(710, 255)	2	Blemish	-	-	-	-	-
162	218D78	(951, 388)	2	-	48-50	4	-	-	-
163	218D78	(949, 622)	2	-	46-48	4	-	-	-
164	218D78	(1053, 109)	2	-	54-56	4	-	-	-
165	219D02	(879, 51)	2	Blemish	-	-	-	-	-
166	219D02	(1051, 423)	2	-	52	-	-	-	36
167	219D02	(1060,1028)	2	-	50	-	12	-	-
168	219D06	(221, 993)	2	-	48	4	-	-	-
169	219D06	(844, 200)	2	-	52-54	4	-	-	-
170	219D08	(106, 173)	2	-	56-58	4	-	-	-
171	219D08	(912, 835)	2	-	46	4	-	-	-
172	219D10	(267, 120)	2-3	(Bit Error)	58	-	-	-	128
173	219D10	(552, 256)	2	-	50	4	-	-	-
174	219D10	(710, 254)	2	Blemish	-	-	-	-	-
175	219D10	(828, 254)	2	-	50-52	4	-	-	-
176	219D10	(994, 857)	2	-	48	4	-	-	-
177	219D14	(302, 95)	2	-	58	4	-	-	-
178	219D14	(327, 173)	2	-	54-56	4	-	-	-
179	219D14	(688, 408)	2	-	46	4	-	-	-
180	219D14	(710, 255)	2	Blemish	-	-	-	-	-

Table 7 (Continued)

Object Number	Pictures Number	Object Coordinates (L,S)	Object Size (pixel)	Camera Blemishes and Local Maximums	Object Background (DN)	Object Brightness above Background (DN) (1-10)	(11-20)	(21-30)	(<30)
181	219D14	(811, 688)	2	-	44-46	4	-	-	-
182	219D14	(879, 51)	2	Blemish	-	-	-	-	-
183	219D14	(985, 294)	2	-	50	4	-	-	-
184	219D16	(112, 116)	2	-	58-60	-	-	30	-
185	219D16	(455, 366)	2	-	48-50	4	-	-	-
186	219D16	(471, 551)	2	0	44-46	-	-	-	48
187	219D16	(575, 408)	2	0	46	4	-	-	-
188	219D16	(636, 400)	3	(Random Error)	-	-	-	-	-
189	219D16	(710, 255)	2	Blemish	-	-	-	-	-
190	219D16	(758, 549)	2	-	44-46	10	-	-	-
191	219D16	(881,1102)	2	-	50-52	6	-	-	-
192	219D16	(1001, 790)	2	-	48	8	-	-	-
193	219D18	(93, 340)	2	-	54-56	4	-	-	-
194	219D18	(814,1069)	2	-	48-50	4	-	-	-
195	219D18	(1015,1135)	2	-	52	4	-	-	-
196	219D18	(1103, 642)	2	-	50	-	18	-	-
197	219D22	(488, 105)	2	-	58-60	4	-	-	-
198	219D22	(617,1145)	2	-	48	4	-	-	-
199	219D22	(898, 207)	2	-	52-54	4	-	-	-
200	219D25	(130, 572)	2	-	48	6	-	-	-
201	219D25	(154, 696)	2	-	50	-	12	-	-
202	219D25	(162, 825)	2	-	50	4		-	-
203	219D25	(177, 585)	2	-	46	-	-	-	34
204	219D25	(184, 516)	2	-	46	10	-	-	-
205	219D25	(310, 614)	3	(Bit Error)	46-48	-	-	30	-
206	219D25	(305,1141)	2	-	52	6	-	-	-
207	219D25	(357, 225)	2	-	42-44	4	-	-	-
208	219D25	(431, 73)	2	-	40-42	-	18	-	-
209	219D25	(541, 672)	2	Blemish	-	-	-	-	-
210	219D25	(568, 673)	2	-	44	10	-	-	-

Table 7 (Continued)

Object Number	Pictures Number	Object Coordinates (L,S)	Object Size (pixel)	Camera Blemishes and Local Maximums	Object Background (DN)	Object Brightness above Background (DN) (1-10)	(11-20)	(21-30)	(<30)
211	219D25	(615, 561)	2	-	40	-		-	48
212	219D25	(720, 368)	2	-	42	-	-	30	-
213	219D25	(881, 171)	2	-	42-44	6	-	-	-
214	219D25	(929, 228)	2	-	42	-	12	-	-
215	219D25	(936, 403)	2	-	42	-	18	-	-
216	219D25	(985, 994)	2	-	48	6	-	-	-
217	219D25	(994, 964)	2	-	46-48	-	14	-	-
218	219D25	(1015, 708)	2	Blemish	-	-	-	-	-
219	219D29	(501, 557)	3	Blemish	-	-	-	-	-
220	219D30	(572,1045)	2	-	46	4	-	-	-
221	219D30	(673,1129)	2	-	48-50	6	-	-	-
222	219D30	(735,1005)	2	-	46	4	-	-	-
223	219D30	(936, 737)	2	-	46-48	4	-	-	-
224	219D30	(996, 869)	2	-	48-50	4	-	-	-
225	219D30	(1006,1022)	2	-	50-52	4	-	-	-
226	219D30	(1027, 441)	2	-	50-52	4	-	-	-
227	219D30	(1027,1129)	2	-	52	4	-	-	-
228	219D30	(1028, 285)	2	-	52-54	4	-	-	-
229	219D30	(1073, 628)	2	-	50-52	4	-	-	-
230	219D30	(1072, 940)	2	Reseau	-	-	-	-	-
231	219D30	(1075, 939)	2	Reseau	-	-	-	-	-
232	219D31	(213, 671)	2	-	48	-	12	-	-
233	219D31	(358, 227)	2		42-44	4	-	-	-
234	219D31	(462, 343)	2-3	(Random Error)	-	-	-	-	-
235	219D31	(493, 279)	2	-	40-42	-	16	-	-
236	219D31	(632, 529)	2	-	40-42	4	-	-	-
237	219D31	(1042, 397)	2	-	42	-	16	-	-
238	219D31	(1038, 711)	2	-	42-44	4	-	-	-
239	219D31	(1049, 914)	2	-	44	-	-	-	36
240	219D31	(1077,1042)	2	-	46-48	-	-	28	-

Table 7 (Continued)

Object Number	Pictures Number	Object Coordinates (L,S)	Object Size (pixel)	Camera Blemishes and Local Maximums	Object Background (DN)	Object Brightness above Background (DN) (1-10)	(11-20)	(21-30)	(<30)
241	219D32	(84,1116)	2	-	54-56	4	-	-	-
242	219D32	(143, 691)	2	-	50	4	-	-	-
243	219D32	(473,1025)	2	-	46-48	4	-	-	-
244	219D32	(871,1099)	2	-	50-52	4	-	-	-
245	219D32	(886, 536)	2	-	46-48	8	-	-	-
246	219D32	(1028, 808)	2	-	50	10	-	-	-
247	219D32	(1088, 602)	2	-	50-52	4	-	-	-
248	219D33	(522, 331)	2	-	44	8	-	-	-
249	219D33	(582, 741)	2	-	44-46	4	-	-	-
250	219D33	(674, 996)	2-8	Blemish	-	-	-	-	-
251	219D33	(706,1151)	2	-	50-52	4	-	-	-
252	219D33	(792,1158)	2	-	50-52	4	-	-	-
253	219D33	(741, 797)	2	Blemish	-	-	-	-	-
254	219D33	(885, 607)	2	Blemish	-	-	-	-	-
255	219D34	(325, 983)	2	-	44-46	-	14	-	-
256	219D34	(654, 548)	2	-	44-46	4	-	-	-
257	219D34	(730, 643)	2	-	44	4	-	-	-
258	219D34	(764, 374)	2	Blemish	-	-	-	-	-
259	219D34	(843, 866)	2	-	46-48	4	-	-	-
260	219D34	(969, 830)	2	-	48-50	-	14	-	-
261	219D34	(999, 630)	2	-	48-50	10	-	-	-
262	219D37	(705,1069)	2	-	48-50	4	-	-	-
263	219D37	(741, 797)	2	Blemish	-	-	-	-	-
264	219D37	(1006,1171)	3	Blemish	-	-	-	-	-
265	219D38	(229,1121)	2	-	50-52	4	-	-	-
266	219D38	(582,1008)	2	-	46	4	-	-	-
267	219D38	(684,188)	2	-	54-56	4	-	-	-
268	219D38	(1087, 646)	2	-	50	4	-	-	-
269	219D38	(1096, 706)	2	-	50	4	-	-	-
270	219D39	(267, 529)	2	-	46	6	-	-	-

Table 7 (Continued)

Object Number	Pictures Number	Object Coordinates (L,S)	Object Size (pixel)	Camera Blemishes and Local Maximums	Object Background (DN)	Object Brightness above Background (DN) (1-10)	(11-20)	(21-30)	(<30)
271	219D39	(674, 996)	2	Blemish	-	-	-	-	-
272	219D39	(741, 797)	2	Blemish	-	-	-	-	-
273	219D40	(415, 804)	2	-	44-46	-	16	-	-
274	219D40	(764, 375)	2	Blemish	-	-	-	-	-
275	219D40	(815,1132)	2	-	50	4	-	-	-
276	219D40	(1032,1006)	2	-	50-52	4	-	-	-
277	219D43	(193, 213)	2	-	44	-	-	-	32
278	219D44	(131,1148)	3	-	52	4	-	-	-
279	219D44	(133,1198)	2	-	52-54	4	-	-	-
280	219D44	(920, 179)	2	-	54	4	-	-	-
281	219D47	(501, 557)	2-4	Blemish	-	-	-	-	-
282	219D47	(725, 362)	2	Blemish	-	-	-	-	-
283	219D47	(863, 642)	2	Blemish	-	-	-	-	-
284	319D47	(887, 216)	2	-	42-44	4	-	-	-
285	219D47	(1018,1165)	2-3	Blemish	-	-	-	-	-
286	219D48	(238,1115)	2	-	50-52	4	-	-	-
287	219D49	(1094,1175)	2	Blemish	-	-	-	-	-
288	219D50	(887, 438)	2	-	48	4	-	-	-
289	219D50	(1048, 554)	2	-	50	-	-	-	48
290	219D53	(501, 557)	2-6	Blemish	-	-	-	-	-
291	219D53	(540, 673)	2	Blemish	-	-	-	-	-
292	219D53	(725, 363)	2	Blemish	-	-	-	-	-
293	219D53	(837, 917)	2	Blemish	-	-	-	-	-
294	219D53	(957, 628)	2	Blemish	-	-	-	-	-
295	219D53	(1006,1171)	2	Blemish	-	-	-	-	-
296	219D53	(1018, 793)	2	-	44-46	4	-	-	-
297	219D53	(1049, 888)	2	-	46-48	4	-	-	-
298	219D53	(1094,1176)	2	Blemish	-	-	-	-	-
299	219D53	(1122, 381)	2	-	44-46	4	-	-	-
300	219D54	(624,1189)	2	-	50-52	4	-	-	-

Table 7 (Continued)

Object Number	Pictures Number	Object Coordinates (L,S)	Object Size (pixel)	Camera Blemishes and Local Maximums	Object Background (DN)	Object Brightness above Background (DN) (1-10)	(11-20)	(21-30)	(<30)
301	219D54	(898, 89)	2	-	58	4	-	-	-
302	219D54	(949, 77)	2	-	58	4	-	-	-
303	219D54	(1093, 476)	2	-	52-54	4	-	-	-
304	219D57	(428, 535)	2	-	44-46	4	-	-	-
305	219D57	(428, 544)	3	Reseau	-	-	-	-	-
306	219D57	(523, 529)	2	Blemish	-	-	-	-	-
307	219D57	(773, 724)	2	-	42	4	-	-	-
308	219D57	(848,1165)	2	-	50-52	4	-	-	-
309	219D57	(965, 523)	2	Blemish	-	-	-	-	-
310	219D58	(748, 692)	2	-	44	6	-	-	-
311	219D58	(796, 940)	2	-	46-48	4	-	-	-
312	219D58	(1020, 952)	2	-	50	-	-	-	36
313	219D58	(1024, 322)	2	-	52	4	-	-	-
314	219D58	(1027, 531)	2	-	50-52	4	-	-	-
315	219D58	(1027, 352)	2	-	52-54	8	-	-	-
316	219D58	(1035, 818)	2	-	50-52	10	-	-	-
317	219D58	(1046, 859)	2	-	50-52	4	-	-	-
318	219D58	(1044,1040)	2	-	52	4	-	-	-
319	219D59	(501, 557)	2-3	Blemish	-	-	-	-	-
320	219D60	(805, 801)	2	-	46	8	-	-	-
321	219D60	(900, 178)	2	Blemish	-	-	-	-	-
322	219D60	(985,1004)	2	-	50	4	-	-	-
323	219D60	(1047, 234)	2	-	54	4	-	-	-
324	219D60	(1052, 815)	2	-	50-52	4	-	-	-
325	219D63	(350, 331)	2	-	42	6	-	-	-
326	219D63	(438, 301)	2	Blemish	-	-	-	-	-
327	219D63	(863, 643)	2	-	42-44	4	-	-	-
328	219D63	(885, 606)	4	Blemish	-	-	-	-	-
329	219D63	(965, 523)	2	Blemish	-	-	-	-	-
330	219D63	(1016,1165)	2	Blemish	-	-	-	-	-

Table 7 (Continued)

Object Number	Pictures Number	Object Coordinates (L,S)	Object Size (pixel)	Camera Blemishes and Local Maximums	Object Background (DN)	Object Brightness above Background (DN) (1-10)	(11-20)	(21-30)	(<30)
331	219D64	(502,1186)	2	-	50-52	-	-	22	-
332	219D64	(517,1180)	2	-	50-52	8	-	-	-
333	219D64	(698,1161)	2	-	48-52	4	-	-	-
334	219D64	(715, 738)	2	-	44	4	-	-	-
335	219D64	(884,1015)	2	-	50	4	-	-	-
336	219D64	(916, 197)	2	-	54-56	6	-	-	-
337	219D64	(1059, 655)	2	-	50-52	4	-	-	-
338	219D64	(1095, 410)	2	-	52-54	4	-	-	-
339	219D67	(772, 338)	2	-	40-42	-	12	-	-
340	219D67	(863, 641)	2	Blemish	-	-	-	-	-
341	219D67	(957, 628)	2	Blemish	-	-	-	-	-
342	219D67	(1034, 468)	2	-	42	-	20	-	-
343	219D67	(1061, 177)	2	-	44-46	4	-	-	-
344	219D68	(158,1185)	2	-	52	4	-	-	-
345	219D68	(218, 857)	2	-	48	-	-	-	38
346	219D68	(273,1136)	2	-	50-52	4	-	-	-
347	219D68	(301, 982)	2	-	48-50	8	-	-	-
348	219D68	(455, 949)	2	-	46-48	-	-	-	34
349	219D68	(851, 638)	2	-	46	4	-	-	-
350	219D68	(1035, 784)	2	-	50-52	4	-	-	-
351	219D68	(1052, 66)	2	-	58-60	4	-	-	-
352	219D69	(438, 301)	2	Blemish	-	-	-	-	-
353	219D69	(885, 606)	2	Blemish	-	-	-	-	-
354	219D69	(1016, 709)	2	Blemish	-	-	-	-	-
355	219D69	(1093,1176)	2	Blemish	-	-	-	-	-

Table 8. Number of Initial Candidate Objects per Radial Interval

Radial Interval (km)	Viking 1 Objects	Viking 2 Objects
1,000- 2,000	0	1
2,000- 3,000	0	0
3,000- 4,000	1	13
4,000- 5,000	4	29
5,000- 6,000	4	40
6,000- 7,000	5	44
7,000- 8,000	6	35
8,000- 9,000	5	39
9,000-10,000	9	34
10,000-11,000	4	30
11,000-12,000	3	19
12,000-13,000	0	15
13,000-14,000	3	15
14,000-15,000	2	12
15,000-16,000	1	7
16,000-17,000	3	7
17,000-18,000	1	3
18,000-19,000	3	4
19,000-20,000	0	2
20,000-21,000	0	1
21,000-22,000	0	1
22,000-23,000	0	2
23,000-24,000	0	0
24,000-25,000	0	1
25,000-26,000	0	0
26,000-27,000	0	0
27,000-28,000	0	0
28,000-29,000	0	0
29,000-30,000	0	1
	54	355

Table 9. Description of the Satellite Correlation Analysis

Step	Description of Each Step
1.	Choose a reference time t_o mid-way in the Viking approach picture time sequence and define it as the observing time appropriate to the ideal space search analysis.
2.	Choose a particular point (R_o, Θ_o) in the ideal space from which to initiate the search procedure.
3.	Project in time and space all initial candidate object coordinates (L,S) into their ideal space coordinates (R, Θ).
4.	Select only those candidate objects within ±500 km radial distance and ±20° angular displacement of the ideal space search point (R_o, Θ_o).
5.	Time transform the ideal point (R_o, Θ_o) into the picture number frames of each selected candidate object and calculate the (L_o, S_o) value of the ideal point in these picture number frames.
6.	For each picture number in step 5, compute the distances d_i between the ideal point (L_o, S_o) and each selected candidate object (L_i, S_i) that occurs in the picture.
7.	Repeat steps 5-6 for all picture numbers containing selected candidate objects and build up a set of values $[d_i]$ associated with the ideal space point (R_o, Θ_o).
8.	Order the set of values $[d_i]$ and determine the five smallest values of d_i [i.e., the five candidate objects nearest the point (R_o, Θ_o)].
9.	Calculate the quantity $(255-d_i)$ for each of the five values (ignoring negative values) and store them in order of decreasing values in the arrays denoted by A, B, C, D, E, where the array elements are those corresponding to the location (R_o, Θ_o) in the two-dimensional (rectangular) ideal space.
10.	Repeat the steps 2-9 for each point in the ideal space.
11.	Set a threshold on the arrays A, B, C, D, and E by deleting all information larger than 30 pixel error in object space coordinates (i.e., subtract 225 from the average and ignore all negative values).
12.	Display separately in the two-dimensional (rectangular) ideal space the new arrays [X = A + B, Y = X + C, Z = Y + Z, and W = Z + E] and produce pixel listing and histograms (frequency distribution diagrams) of these new arrays.

Table 9 (Continued)

Step	Description of Each Step
13.	Use the results of step 12 to manually locate correlated maximums in the two-dimensional (rectangular) ideal space.
14.	Identify the initial candidate points that produce the correlated maximums.
15.	Verify these identified candidate points are satellite by examining their time and space projection into all picture frames and checking that their pixel locations and signatures are consistent with the view and camera parameters of each picture frame.

Table 10. Phobos in the Viking 1 Approach Pictures

Object Number	Picture Number	Camera A/B	Filter	Exposure (ms)	Relative Sensitivity†	Phobos Above Background (DN)	Spacecraft Range (km)	Satellite Imaged
3	169C26	A	VLT	407.3	2.02	4	563,591	Phobos
	C30	A	GRN	67.88	0.92	<2	563,545	-
	C32	A	RED	135.8	0.68	-	563,521	-
15	169C61	A	VLT	407.3	2.02	8	466,265	Phobos
	C65	A	GRN	67.88	0.92	2-4	466,218	Phobos
	C67	A	RED	135.8	0.68	<2	466,195	-
43	170C30	A	MBL	50.91	0.91	4	348,628	Phobos
46	170C32	A	VLT	407.3	2.02	8	348,604	Phobos

†Relative sensitivity is defined in Table 5.

FIGURE CAPTIONS

Figure 1. Viking 1 Approach Picture. A print of the Viking 1 approach picture number 170C34 is shown that has been geometrically corrected and filtered to enhance geological details on Mars. On the planet, circles at constant latitudes of 0°, -30°, -60° and -85° are indicated. In the equatorial plane circular orbits with radii between 5,000 and 10,000 km are shown at a 1,000 km spacing.

Figure 2. Screening of the Image Data. The screening process applied to the Viking Orbiter EDR data for the approach pictures in order to develop an initial list of satellite candidate objects is illustrated.

Figure 3. Possible Viking 1 Initial Candidate Objects. A print of the Viking 1 approach picture 170C32 is shown that has been enhanced to show the background brightness levels in the image. The locations of possible initial candidate objects, numbered both within and beyond the planetary disk, are shown in order to facilitate manual screening. Object number 347 (upper left) is Phobos.

Figure 4. Possible Viking 2 Initial Candidate Objects. A print of the Viking 2 approach picture 218D24 is shown that has been enhanced to show the background brightness levels in the image. This image shows greater background variation than the Viking 1 picture of Figure 3. The locations of possible initial candidate objects, numbered both within and beyond the planetary disk, are shown in order to facilitate manual screening.

Figure 5. First Order Navigation Processing of the Initial Candidate Object Data. The procedure applied to geometrically correct and navigate the initial candidate object data is illustrated.

Figure 6. Error Ellipse Diagrams for the Viking 1 Initial Candidate Objects. Error ellipses are shown in the ideal coordinate frame for the initial candidate objects with radial distances of 8001 to 10,000 km (downward vertical axis, 3 km/pixel scale) from Mars and with circular longitude coordinates from 0 to 360 degrees (horizontal axis, 0.5 degrees/pixel scale) around Mars. The transparent overlay identifies each long needle-like error ellipse with the object number of its initial candidate object given in Table 6.

Figure 7. Error Ellipse Intersections for the Viking 1 Initial Candidate Objects. A closeup of the two intersections of the error ellipses in Figure 6 is shown, where the first three overlay brightness contours separated by 10 DN are indicated.

Figure 8. Correlation Diagram for Phobos in the Viking 1 Approach Pictures. The correlation diagram is shown for the primary intersections of the error ellipses in Figure 6. The smallest contour, indicating the most probable location of Phobos, provides an orbital radius estimate of 9374 kilometers. See text for discussion.

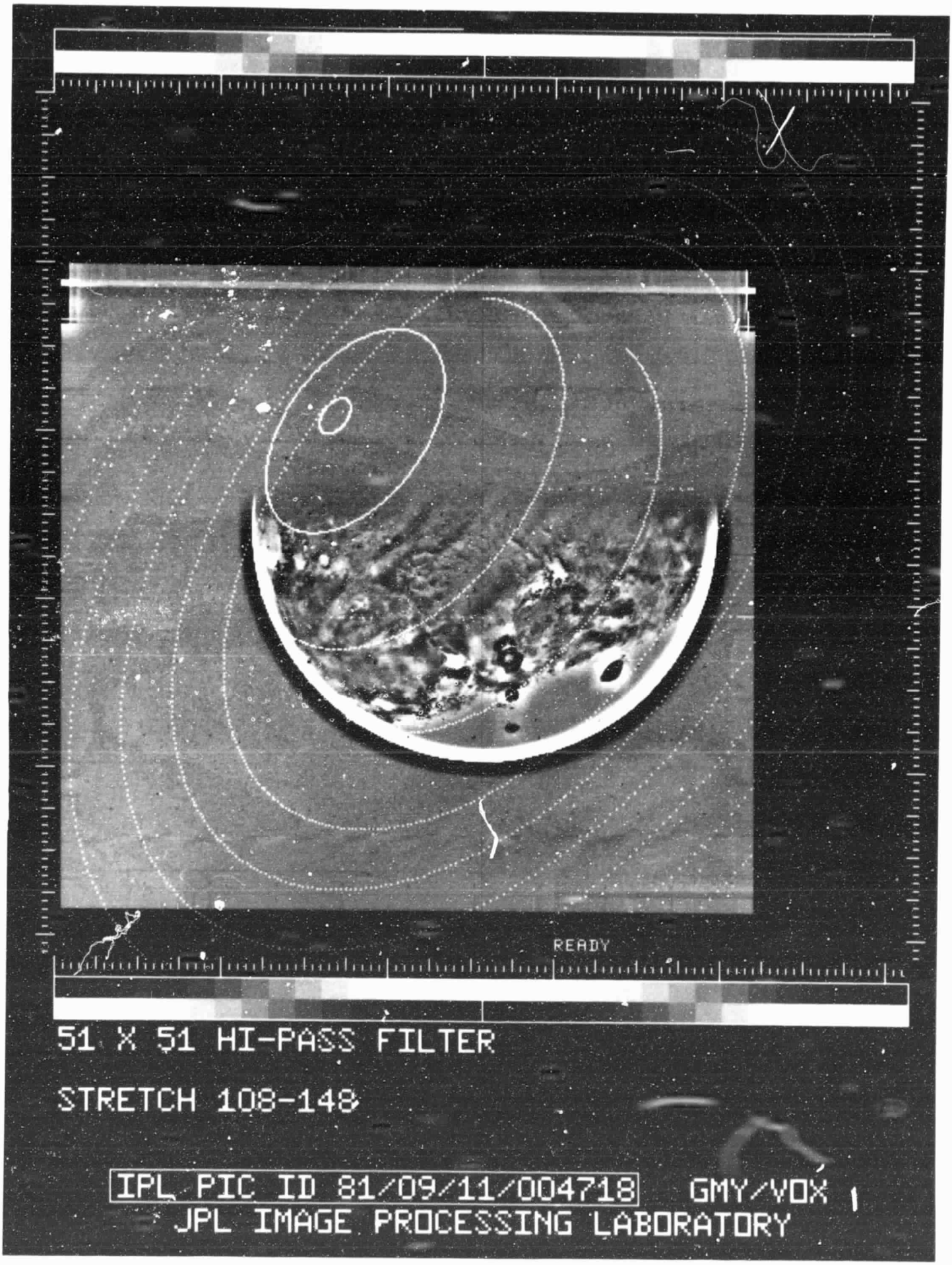
READY
51 X 51 HI-PASS FILTER
STRETCH 108-148
IPL PIC ID 81/09/11/004718 GMY/VOX
JPL IMAGE PROCESSING LABORATORY

Figure 1

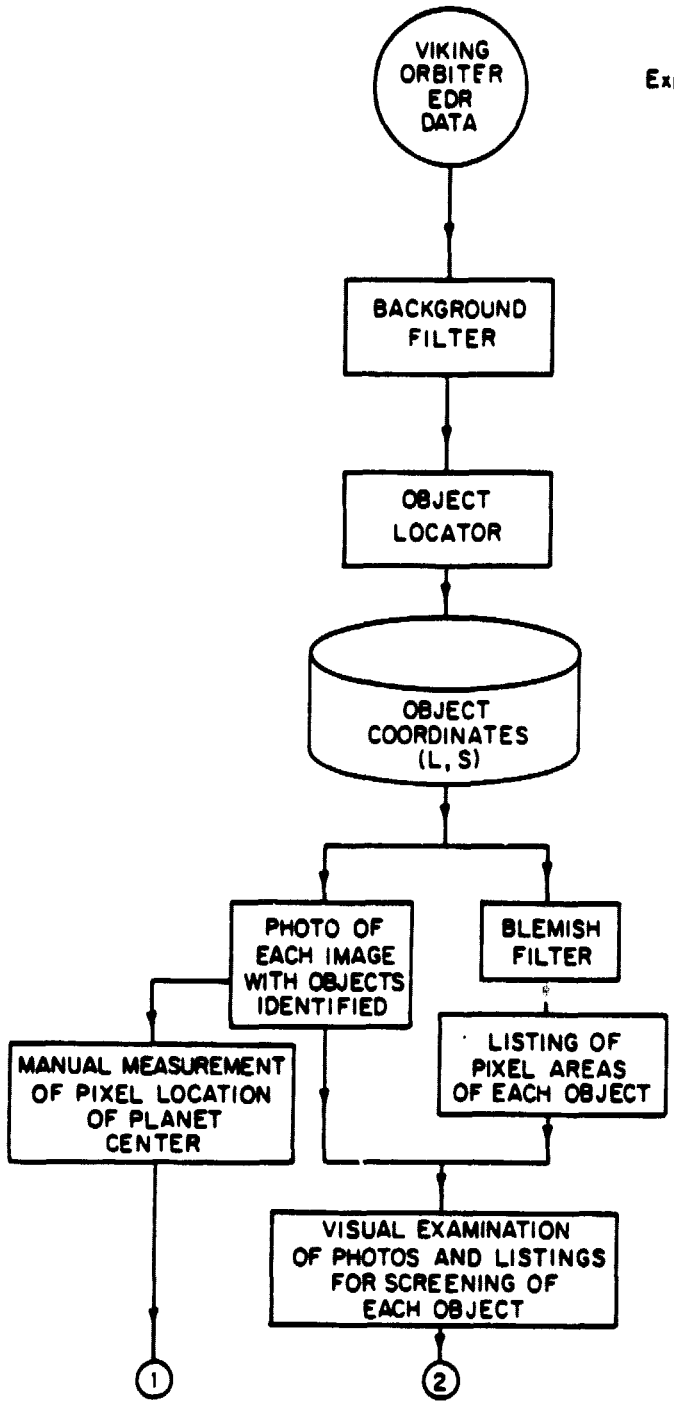

Figure 2

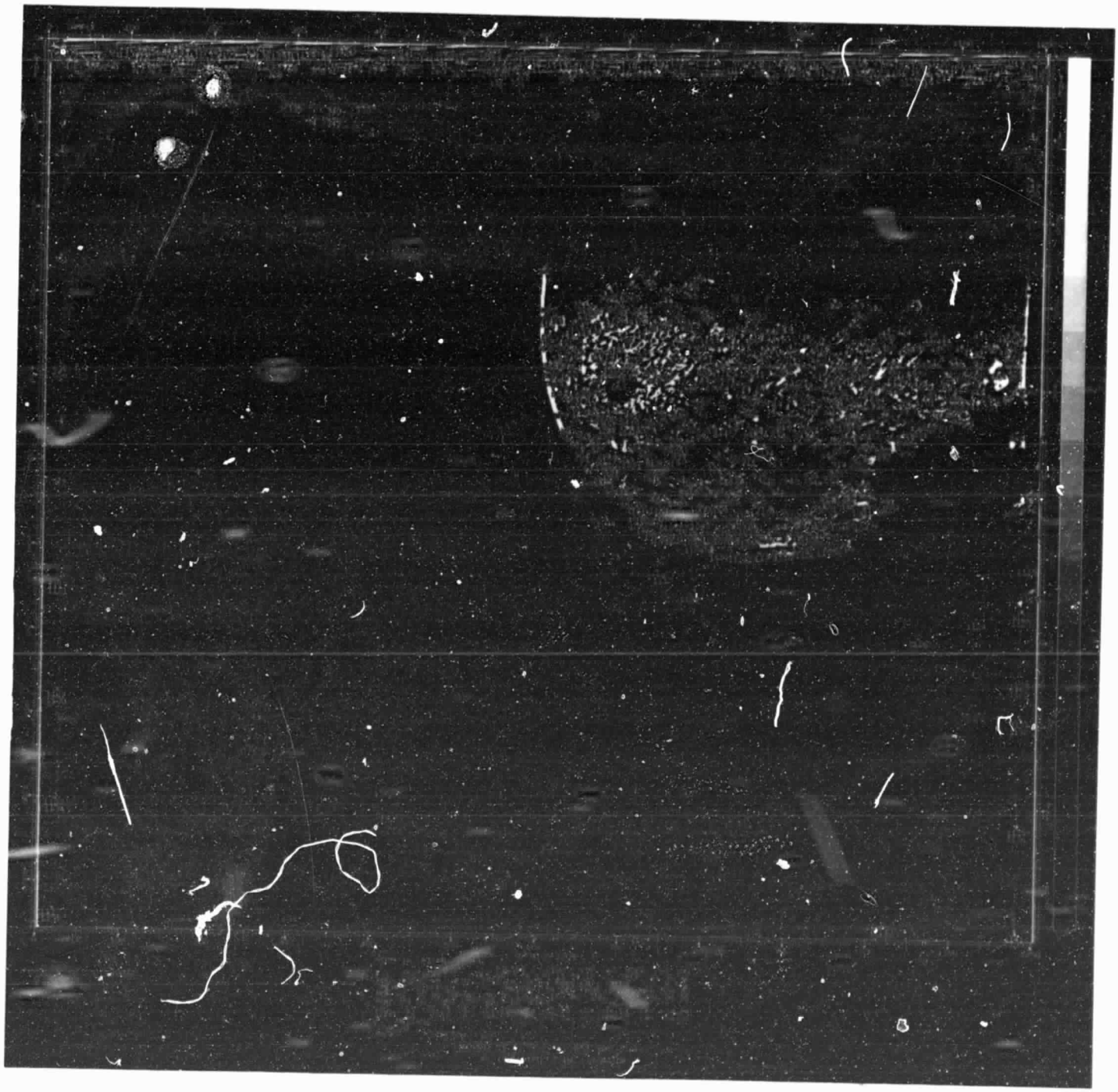

Figure 3

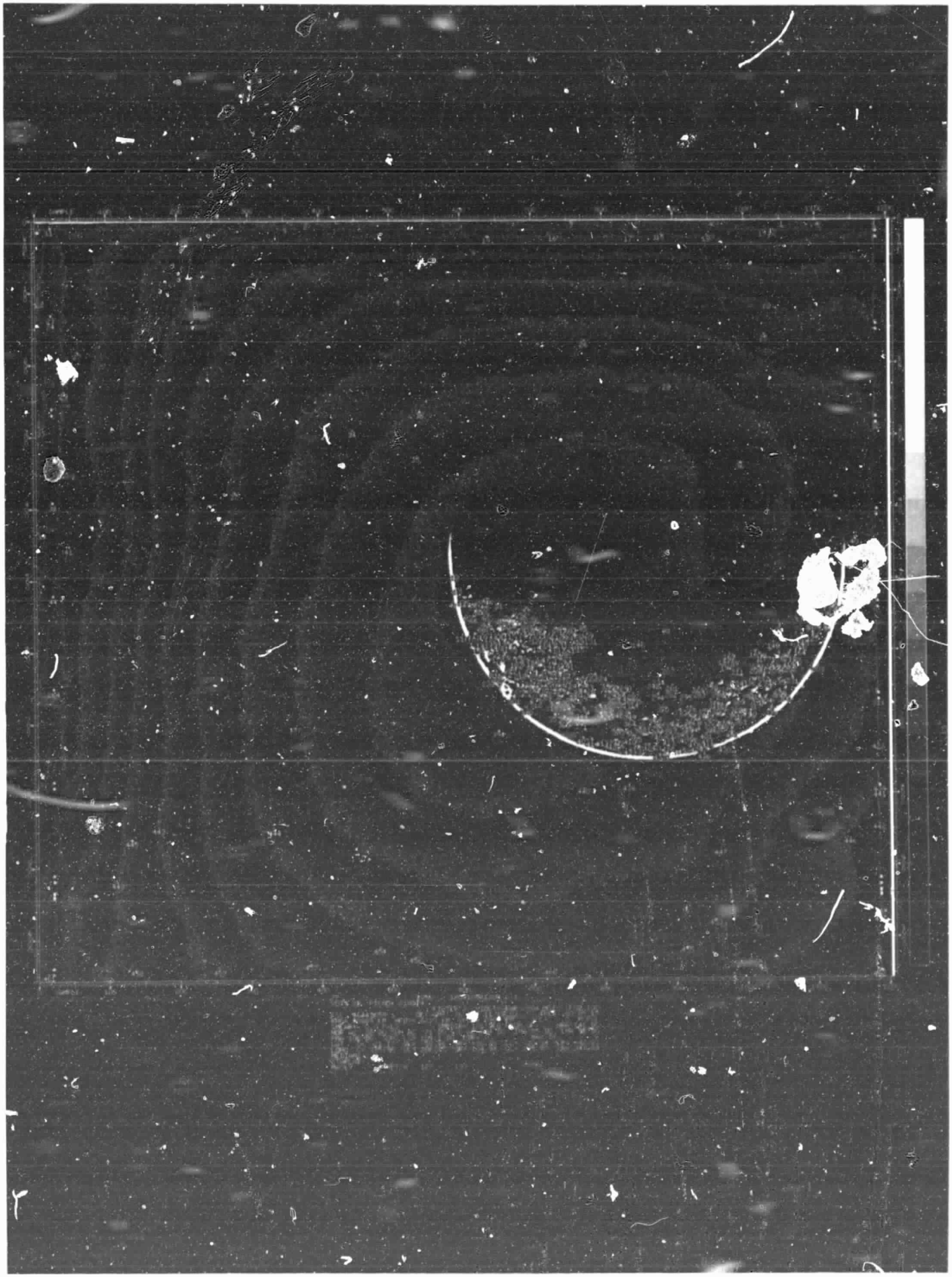

Figure 4

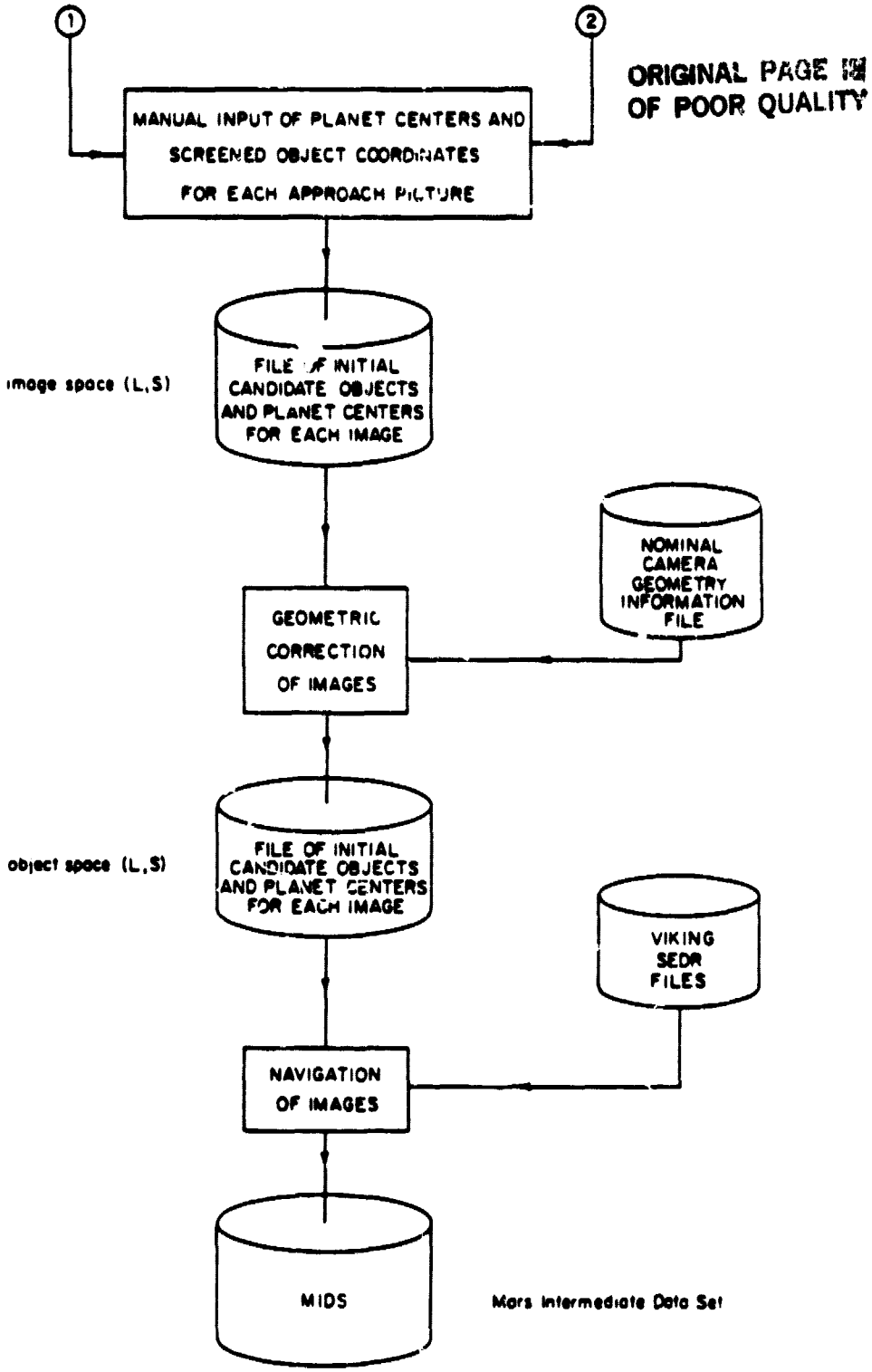

Figure 5

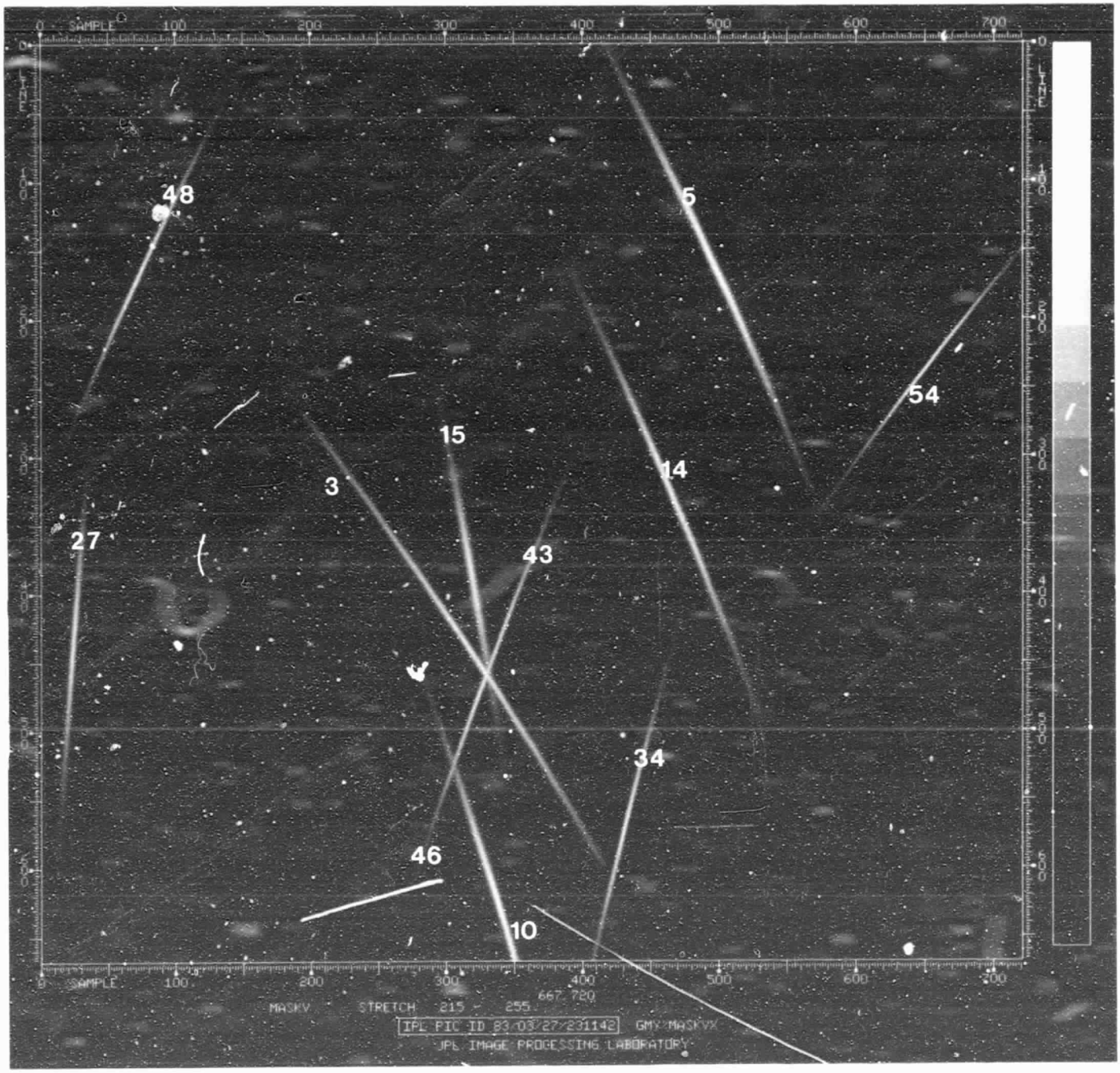

Figure 6

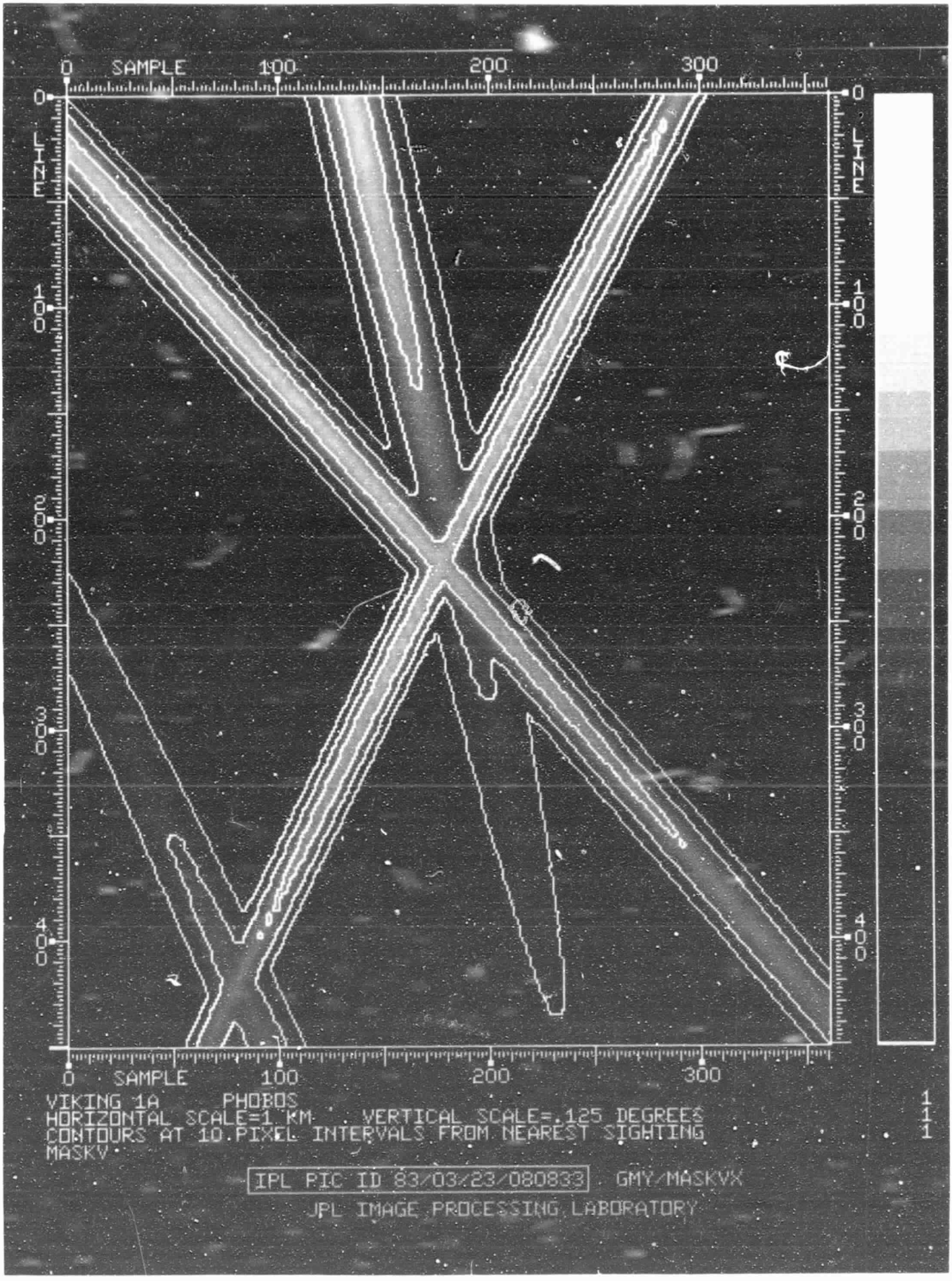
0 SAMPLE 100 200 300
LINE
SAMPLE
VIKING 1A PHOBOS
HORIZONTAL SCALE=1 KM VERTICAL SCALE=.125 DEGREES
CONTOURS AT 10.PIXEL INTERVALS FROM NEAREST SIGHTING
MASKV
IPL PIC ID 83/03/23/080833 GMY/MASKVX
JPL IMAGE PROCESSING LABORATORY

Figure 7

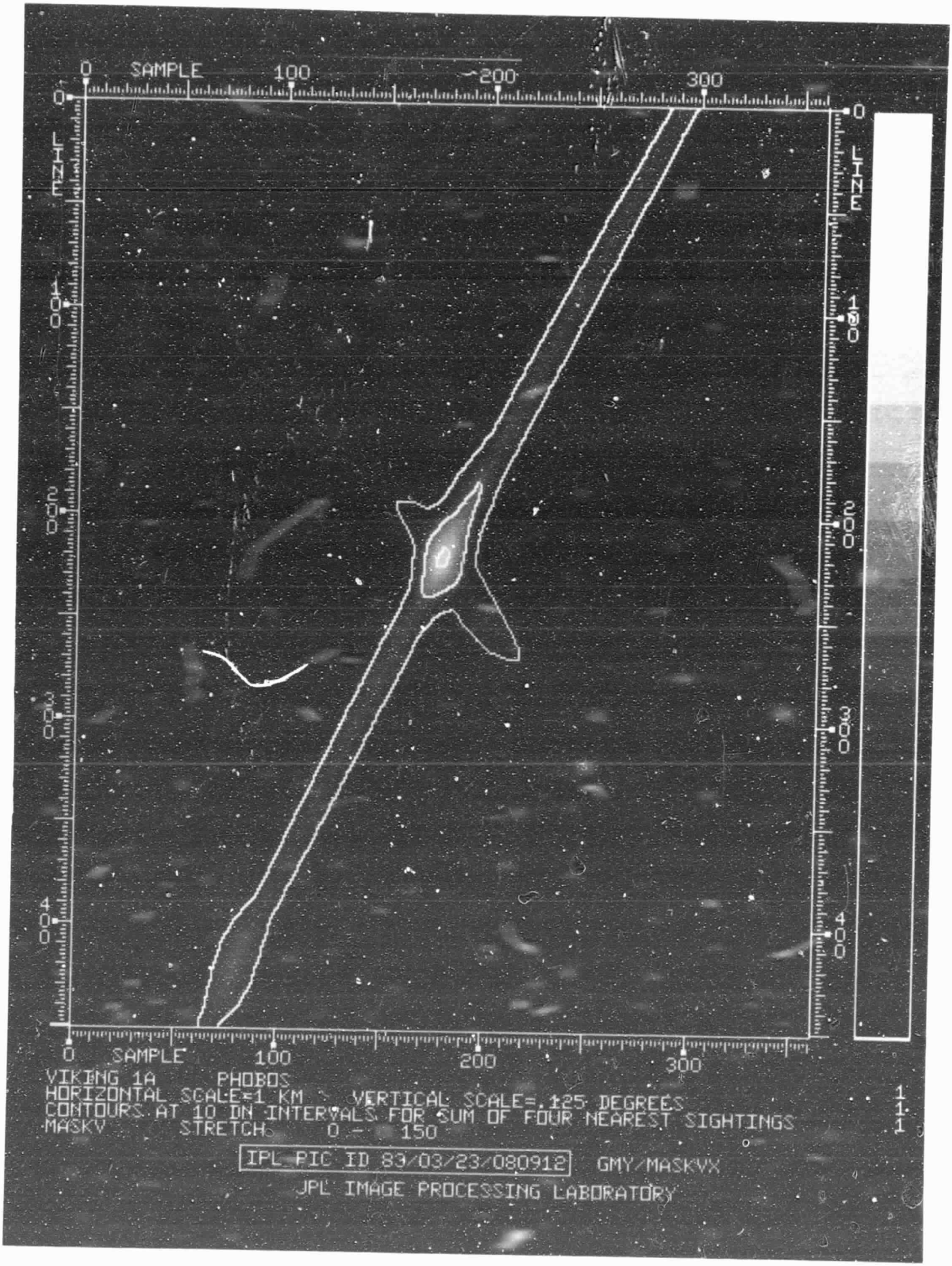
0 SAMPLE 100 200 300
LINE
0 100 200 300 400
VIKING 1A PHOBOS
HORIZONTAL SCALE=1 KM VERTICAL SCALE=.125 DEGREES
CONTOURS AT 10 DN INTERVALS FOR SUM OF FOUR NEAREST SIGHTINGS
MASKV STRETCH 0 - 150
IPL PIC ID 83/03/23/080912 GMY/MASKVX
JPL IMAGE PROCESSING LABORATORY

Figure 8